Published August 30, 2010

Subgroup II PAK-mediated phosphorylation regulates Ran activity during mitosis

Guillaume Bompard,[1,2] Gabriel Rabeharivelo,[1,2] Marie Frank,[1,2] Julien Cau,[1,3] Claude Delsert,[1,2,4] and Nathalie Morin[1,2]

[1]Universités Montpellier 2 et 1, IFR122, 34293 Montpellier, France
[2]Centre de Recherche de Biochimie Macromoléculaire, Centre National de la Recherche Scientifique, UMR 5237, 34293 Montpellier, France
[3]Institut de Génétique Humaine, Centre National de la Recherche Scientifique UPR1142, 141, 34396 Montpellier, France
[4]IFREMER Laboratoire de Génétique et Pathologie, 17390 la Tremblade, France

Ran is an essential GTPase that controls nucleocytoplasmic transport, mitosis, and nuclear envelope formation. These functions are regulated by interaction of Ran with different partners, and by formation of a Ran-GTP gradient emanating from chromatin. Here, we identify a novel level of Ran regulation. We show that Ran is a substrate for p21-activated kinase 4 (PAK4) and that its phosphorylation on serine-135 increases during mitosis. The endogenous phosphorylated Ran and active PAK4 dynamically associate with different components of the microtubule spindle during mitotic progression. A GDP-bound Ran phosphomimetic mutant cannot undergo RCC1-mediated GDP/GTP exchange and cannot induce microtubule asters in mitotic *Xenopus* egg extracts. Conversely, phosphorylation of GTP-bound Ran facilitates aster nucleation. Finally, phosphorylation of Ran on serine-135 impedes its binding to RCC1 and RanGAP1. Our study suggests that PAK4-mediated phosphorylation of GDP- or GTP-bound Ran regulates the assembly of Ran-dependent complexes on the mitotic spindle.

Introduction

The Ran GTPase modulates nucleocytoplasmic shuttling, bipolar spindle assembly, chromosome segregation, and nuclear envelope reassembly at the end of mitosis (Clarke and Zhang, 2004; Arnaoutov and Dasso, 2005; Goodman and Zheng, 2006; Terry et al., 2007). Ran activity depends on its GTP/GDP cycle, and the subcellular localization of its regulatory enzymes. Indeed, the Ran exchange factor RCC1 is chromatin bound, whereas RanGAP1 and its accessory proteins RanBP1 and RanBP2 are essentially cytoplasmic during interphase. This partitioning restricts Ran-GTP to the nucleus and Ran-GDP to the cytoplasm (Clarke and Zhang, 2008).

Nucleocytoplasmic shuttling is regulated by Ran-GTP binding to its effectors, which belong to the importin and exportin (CRM1) family. Nuclear localization sequence (NLS)–bearing proteins bind the importins in the cytoplasm and are transported into the nucleus where the interaction of Ran-GTP with importin-β releases and activates the NLS cargoes. Importin cargoes include most nuclear proteins, of which some contribute to spindle formation during mitosis (Terry et al., 2007; Clarke and Zhang, 2008). In the nucleus, Ran-GTP also promotes the CRM1 loading of nuclear export sequence (NES)–bearing proteins and their subsequent export to the cytoplasm. When the nuclear envelope breaks down at mitosis, the Ran-GTP/GDP physical compartimentalization is abolished. At this point, Ran activity and function appears to rely on essentially two mechanisms.

The first mechanism is the spatially controlled assembly of protein complexes at specific subcellular localizations. For instance, at the kinetochore region Ran-GTP/CRM1–dependent recruitment of RanGAP1 and RanBP2 is essential for kinetochore–microtubule interactions (Joseph et al., 2004; Arnaoutov et al., 2005), whereas at the centrosome the Ran-GTP/CRM1–dependent recruitment of nucleophosmin regulates unscheduled centrosome duplication (Budhu and Wang, 2005; Wang et al., 2005). Among others, importin-β, which is transported along microtubules (MTs) by dynein (Ciciarello et al., 2004), RanBP1, and centrosomal matrix A-kinase anchoring protein (AKAP450; Keryer et al., 2003) also colocalize and/or are complexed with Ran at the centrosomes.

Correspondence to Nathalie Morin: nathalie.morin@crbm.cnrs.fr

Abbreviations used in this paper: MBP, maltose binding protein; NES, nuclear export sequence; NLS, nuclear localization sequence; PAK, p21-activated kinase; Plk1, polo-like kinase; SAF, spindle assembly factor; wt, wild type.

The Rockefeller University Press $30.00
J. Cell Biol.
www.jcb.org/cgi/doi/10.1083/jcb.200912056

Published August 30, 2010

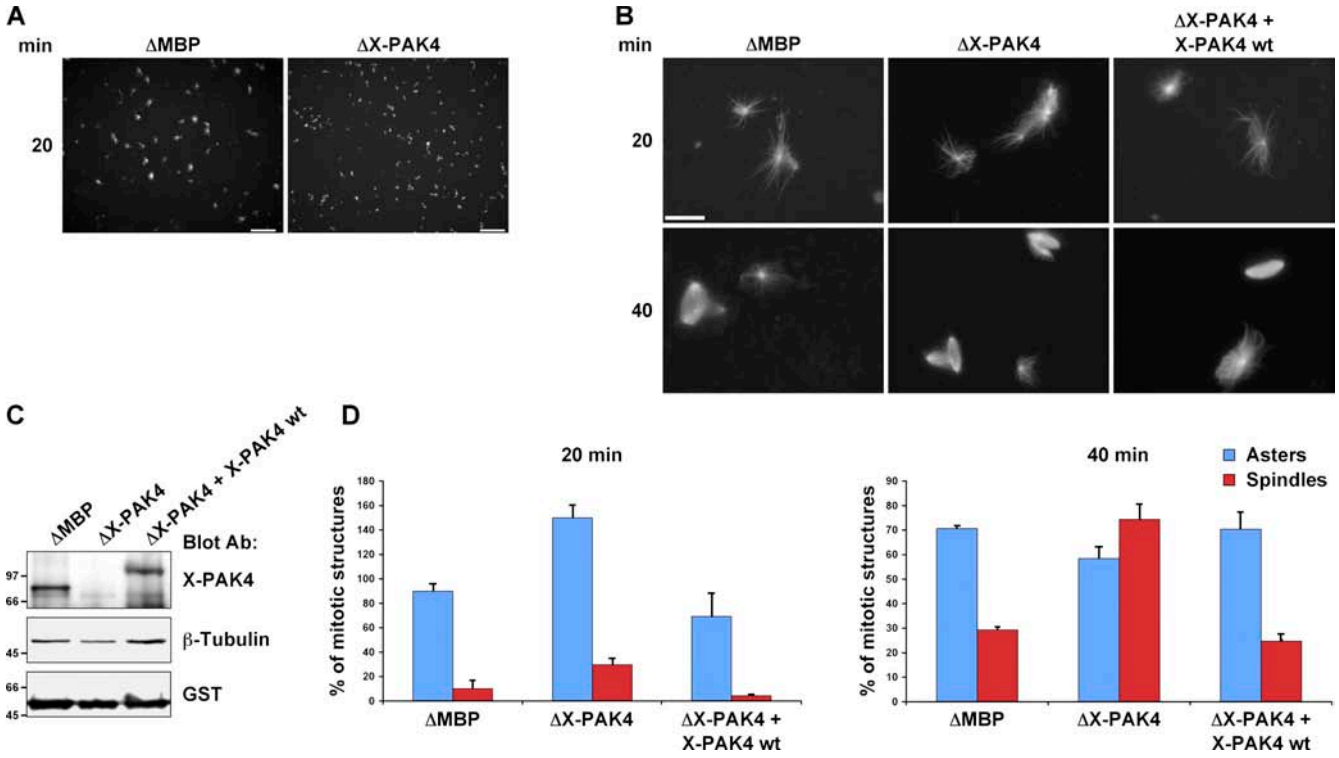

Figure 1. **Ran-GTP–induced MT aster nucleation is enhanced in X-PAK4–depleted CSF extracts.** (A) Asters and mitotic spindle assembly was initiated by addition of 15 µM RanQ69L, either in ΔMBP or ΔX-PAK4 extracts. Representative fluorescent micrograph taken at low magnification showing the abundance of MTs structures formed 20 min after RanQ69L addition. Bar, 100 µm. (B) Representative micrographs of MT structures assembled as in A and after addition of recombinant X-PAK4 for complementation at indicated times. Bar, 25 µm. (C) Extracts treated as in B were analyzed by immunoblot, for X-PAK4 depletion and complementation (X-PAK4 wt) and for recombinant Ran stability (GST). β-Tubulin was used as a loading control. (D) Quantification of the numbers and quality (asters or spindles) formed in the extracts as in B (n = 3, ±SD). Control condition is given an arbitrary 100% value at each time point.

Second, a Ran-GTP diffusible gradient is established, during mitotic spindle assembly, by chromatin-bound RCC1. This gradient, first visualized by Forster resonance energy transfer (FRET) in *Xenopus* egg extracts (Kalab et al., 2002; Caudron et al., 2005; Kaláb et al., 2006), induces a spatially controlled release of spindle assembly factors (SAFs) such as TPX2, from the inhibitory importins (Caudron et al., 2005; Bastiaens et al., 2006). In somatic cells, although the Ran-GTP gradient contributes to spindle establishment during early mitosis, it clearly becomes dispensable at metaphase (Kaláb et al., 2006; Kalab and Heald, 2008).

During mitosis Ran must be differentially regulated in the different complexes present at the same subcellular location. However, neither the localization nor the gradient mechanism fully explains the control of Ran activity, which argues for another level of modulation of the activity of the GTPase. We hypothesized that phosphorylation, one of the chief mechanisms regulating mitotic progression, might control Ran function, as many kinases localize to the centrosome and kinetochore regions during spindle assembly.

The p21-activated kinase (PAK) family is central to many signaling pathways (Arias-Romero and Chernoff, 2008; Molli et al., 2009). This family is commonly divided into subgroups I (PAK1–3) and II (PAK 4–6). PAK4–6 are involved in controlling cross talk and reorganization of the actin and MT cytoskeletons (Cau et al., 2001; Callow et al., 2002). We previously reported that X-PAK4 (although previously called X-PAK5, it is the orthologue of hPAK4, we therefore propose to change its name to X-PAK4) regulates MT dynamics in interphase cells and is associated with spindle MTs in mitosis (Cau et al., 2001). In the present study, we show that Ran is phosphorylated by PAK4 on a unique serine residue at position 135 (Ran Ser135P). Ran Ser135P increases during mitosis and associates with centrosomes from prophase to anaphase and with foci from prophase to metaphase. Later, Ran Ser135P localizes to the central spindle and around the midbody. Strikingly, these localizations reflect the distribution of the active X-PAK4 during mitosis. We found that a GDP-bound Ran phosphomimetic mutant cannot induce MT asters in mitotic-arrested (CSF) *Xenopus* egg extracts because RCC1-mediated GDP/GTP exchange is impeded. PAK4-mediated phosphorylation of Ran reproduces the phosphomimetic mutant-induced phenotype. We further show that phosphorylation of Ran on serine-135 impedes its binding to RCC1 and RanGAP1. Altogether, our findings strongly suggest that PAK4-mediated phosphorylation of GDP- or GTP-bound Ran modulates the assembly of complexes that are required at specific subcellular localizations for Ran to carry out its functions during mitotic progression.

Results

Immunodepletion of X-PAK4 in *Xenopus* egg extracts facilitates induction of MT nucleation centers by Ran

X-PAK4 regulates MT dynamics in interphase and associates with the spindle during mitosis (Cau et al., 2001). To analyze

Published August 30, 2010

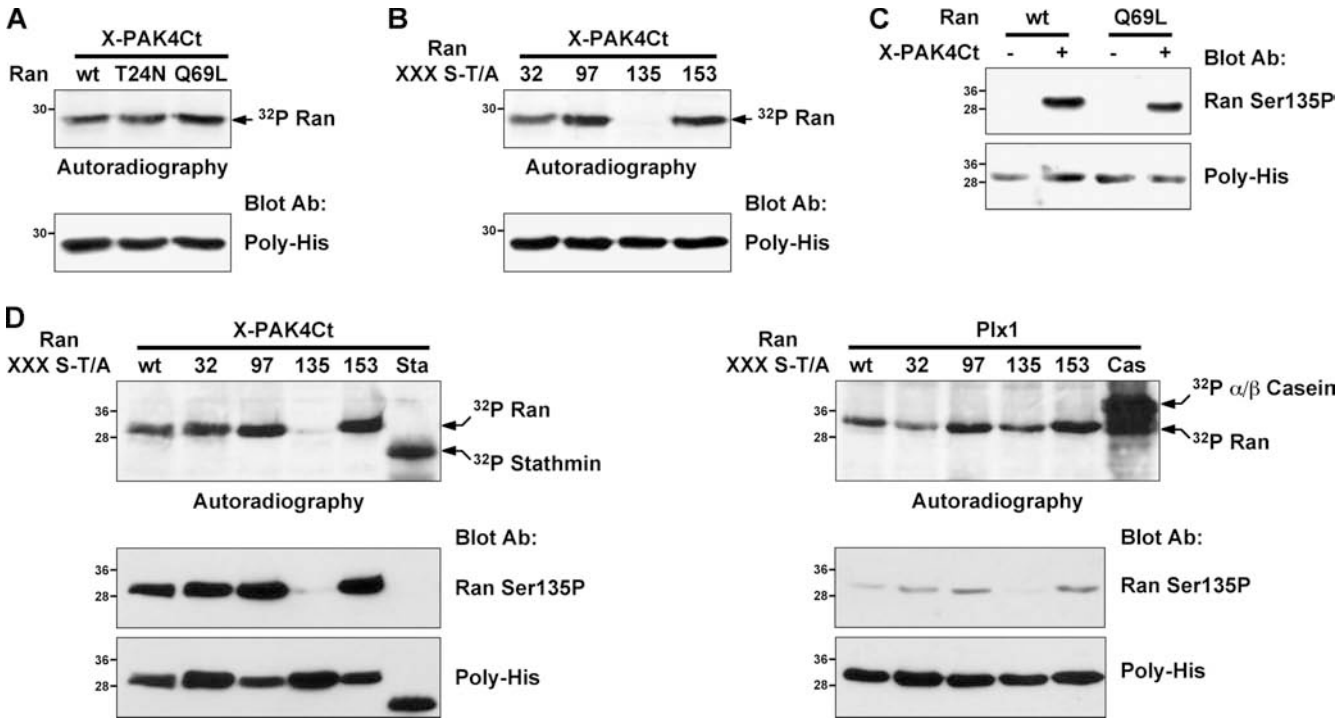

Figure 2. **X-PAK4 phosphorylates Ran on serine-135.** (A and B) Autoradiographies (top panels) and Poly-His immunoblots as loading controls of the same membranes (bottom panels) of in vitro phosphorylation by active X-PAK4Ct of His-tagged wt, T24N, and Q69L Ran mutants (A); and T32A, T97A, S135A, and S153A Ran mutants (B). (C) Immunoblots of the His-tagged Ran wt and Q69L mutant after incubation with (+) or without (−) X-PAK4Ct using Ran Ser135P and Poly-His antibodies. (D) Autoradiographies (top panels), before immunoblots using Ran Ser135P and Poly-His antibodies (bottom panels), of His-tagged Ran mutants and stathmin (Sta) and of α/β casein (Cas) after phosphorylation by X-PAK4Ct (left panels) or Plx1 kinase (right panels). X-PAK4 and Plx matching panels were exposed and processed together for both autoradiography and immunoblots.

whether X-PAK4 regulates mitotic MTs in the absence of centrosomes and chromatin, we used the GDP-bound RanQ69L mutant that can bind but not hydrolyze GTP. This mutant, and others that stabilize the GTP-bound form of Ran, have been extensively used to induce MT asters and spindle-like structures in CSF extracts (Carazo-Salas et al., 1999; Kalab et al., 1999; Ohba et al., 1999; Wilde and Zheng, 1999). After one round of immunodepletion (ΔX-PAK4) the endogenous X-PAK4 was no longer detectable, whereas the control depletion (ΔMBP, using an antibody against maltose binding protein) did not affect the X-PAK4 level. To rescue the phenotype, GST-fused wild-type X-PAK4 (X-PAK4wt) was added to ΔX-PAK4 extract to reconstitute the endogenous level (Fig. 1 C). 20 min after the addition of 15 μM RanQ69L, mitotic asters were induced in both the ΔX-PAK4 and the ΔMBP extracts. Asters formed in the ΔX-PAK4 were smaller and had a brighter center than in ΔMBP, indicating that more MTs were nucleated, and these asters evolved more rapidly into spindle-like structures (Fig. 1, A and B). Quantitative analyses showed that after 20 min, at least twice as many asters were nucleated in the ΔX-PAK4 extract (Fig. 1 D). 40 min after the addition of RanQ69L, the total number of mitotic figures in ΔX-PAK4 and ΔMBP extracts tended to equalize. However, depletion of X-PAK4 was accompanied by an increase of the bipolarization activity, compared with the ΔMBP extract (Fig. 1 D). This phenotype is specific because it is rescued by the addition of recombinant X-PAK4 (Fig. 1, B and D).

Our data suggest an inhibitory effect of X-PAK4 on MT nucleation and stabilization factors induced by GDP-bound RanQ69L. The binding of RanQ69L to the endogenous importin-β in the CSF extract allows the release and the activation of SAFs that promote the assembly and bipolarization of asters (Gruss et al., 2001; Wiese et al., 2001). TPX2, under these conditions, is the most important nucleation factor involved. However, we found no evidence that TPX2 is directly regulated by PAK4-mediated phosphorylation (unpublished data).

X-PAK4 phosphorylates Ran on serine-135

Because Ran-induced MT nucleation and bipolarization are affected upon X-PAK4 depletion, we hypothesized that X-PAK4 could directly regulate Ran. We found, using an in vitro kinase assay, that wild type (wt), T24N (a mutant defective in GTP binding), and Q69L Ran mutants could all be phosphorylated by the active recombinant catalytic domain of X-PAK4 (X-PAK4Ct; Fig. 2 A).

The amino acid sequence of Ran reveals four potential PAK phosphorylation motifs (Zhu et al., 2005; Rennefahrt et al., 2007) at threonine residues 32 and 97 and serine residues 135 and 153. These residues were mutated to alanine (A) and the recombinant Ran mutants were used as a substrate for X-PAK4Ct. All mutants except S135A incorporated γ-[^{32}P]ATP, demonstrating that X-PAK4 phosphorylates in vitro a unique serine at position 135 on Ran (Fig. 2 B). Interestingly, it was previously reported that a small fraction of Ran phosphorylated

Published August 30, 2010

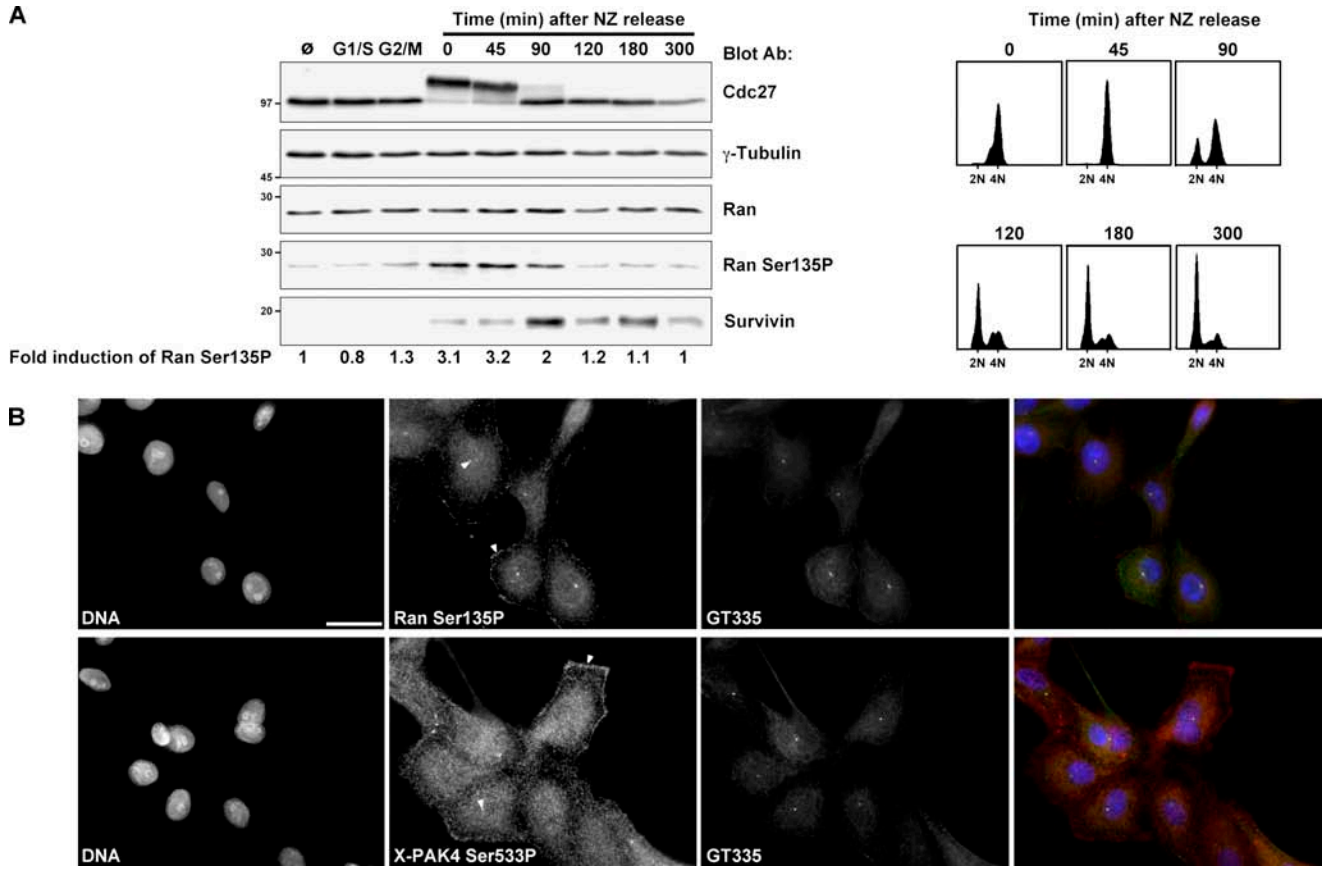

Figure 3. **Ran Ser135P concentration increases during mitosis.** Ran Ser135P shares common subcellular localization with active PAK4. (A, left) Immunoblots of total HeLa cell extracts from asynchronous, G1/S, G2/M, prometaphase (0) and after nocodazole (NZ) release probed for Cdc27, survivin as mitotic markers, γ-tubulin as loading control, Ran and Ran Ser135P. Fold induction of Ran Ser135P is indicated. (A, right) FACS analyses of cells upon NZ release. (B) Localization of Ran Ser135P and active X-PAK4 Ser533P in XL-2 cells during interphase. Cells were stained for DNA immunostained with GT335 and Ran Ser135P or the active forms of subgroup II PAK (X-PAK4 Ser533P). Arrowheads show Ran Ser135P and X-PAK4 Ser533P at centrioles and lamellipodia. Bar, 25 μm.

on serine-135 coprecipitates with polo-like kinase 1 (Plk1) during mitosis in somatic cells (Feng et al., 2006). However, a direct phosphorylation of Ran by Plk1 is unlikely because the sequence surrounding serine-135 does not match the Plk1 consensus phosphorylation site (Nakajima et al., 2003).

To reassess the roles of Plx1 (the *Xenopus* Plk1 orthologue) and X-PAK4 in the phosphorylation of Ran on serine-135, we generated an antibody directed against a peptide surrounding the phosphorylated serine-135 of Ran. The Ran Ser135P antibody only weakly revealed unphosphorylated wt and Q69L mutant Ran on immunoblot analysis (unpublished data). In contrast, after phosphorylation of the recombinant Ran proteins by the X-PAK4Ct, the antibody efficiently detected Ran phosphorylated on serine-135 (RanSer135P; Fig. 2 C).

Next, we compared the phosphorylation patterns of the wt and four Ran mutants after their incubation with active X-PAK4 and Plx1 (Fig. 2 D). Recombinant stathmin and α/β casein were used as substrates for PAK4 and Plx1, respectively, to standardize the specific kinase activities added in the assays. Again, X-PAK4 phosphorylated wt, T32A, T97A, and S153A Ran mutants, but not Ran S135A. The ^{32}P phosphorylation pattern was faithfully mimicked by the Ran Ser135P immunoblot, further confirming the specificity of the antibody. In the equivalent reaction with Plx1 all recombinant Ran proteins were phosphorylated, demonstrating that Plx1 may either target several sites, or a site other than the four mutated residues. A weak Ran Ser135P signal was detected on all but the Ran S135A mutant, indicating that Plx1 can, to some extent, phosphorylate serine-135 (Fig. 2 D). However, this residue is a very poor substrate for Plx1 as opposed to PAK4 because corresponding panels shown for the two kinases were exposed simultaneously. Thus, although unlikely, we cannot completely rule out that Plx1 might phosphorylate serine-135 in vivo. We further studied the phosphorylation of the endogenous Ran on serine-135, upon the expression of constitutively active full-length mutants of mammalian and *Xenopus* PAKs representative of the two subgroups, in HEK293 cells (Fig. S1). Serine-16 phosphorylation of the MT-destabilizing protein stathmin (Stathmin Ser16P), which was used as a substrate for active PAK1 (Wittmann et al., 2004), is also induced by all active subgroup II PAKs tested. In contrast, Ran Ser135P is restricted to cells expressing active subgroup II PAK members. This is an interesting finding because even though both kinase subgroups are differentially regulated, all the PAK4 substrates identified so far are also phosphorylated by PAK1 (Arias-Romero and Chernoff, 2008). In summary, we show here that subgroup II PAKs specifically phosphorylate the Ran GTPase on serine-135

Published August 30, 2010

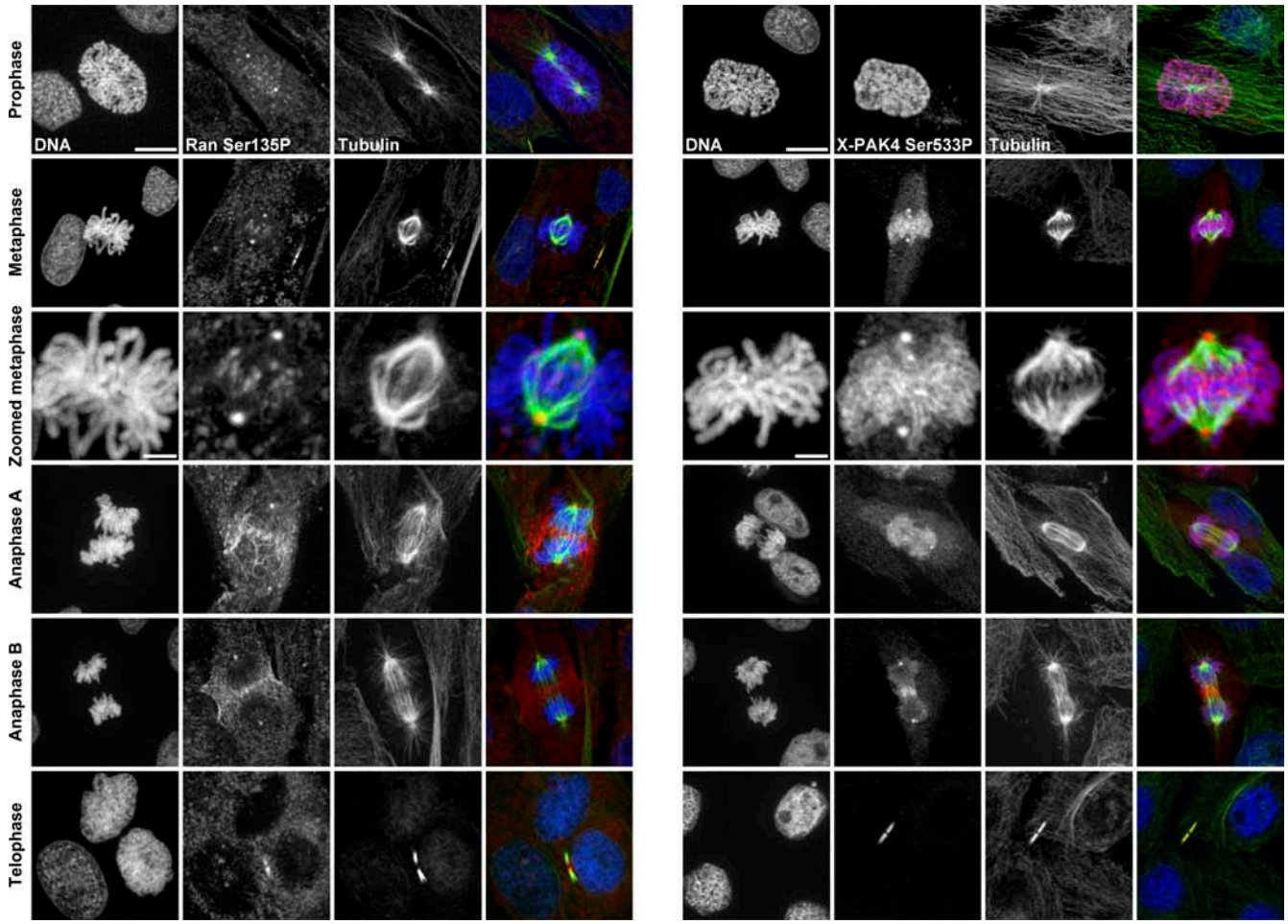

Figure 4. **Ran Ser135P shares common subcellular localization with active PAK4.** Localization of Ran Ser135P and X-PAK4 Ser533P in XL-2 cells during mitosis. Metaphase panels are shown at higher magnification. Cells were stained as in Fig. 3. β-Tubulin was immunostained instead of GT335. Bars, 10 µm (except for zoomed metaphase, 2.5 µm).

Active X-PAK4 and RanSer135P colocalize to specific substructures during mitosis

Next, we asked whether Ran Ser135 phosphorylation is cell cycle dependent. HeLa cells were synchronized in early S phase by a thymidine block followed by treatment with either the Cdk1 inhibitor RO3306 to provoke a G2/M arrest or nocodazole to induce a prometaphase arrest. Upon nocodazole release, cells were allowed to proceed through mitosis. Cell DNA content and total cell lysates were analyzed at the indicated time points by FACS and immunoblot, respectively (Fig. 3 A). Total Ran is constant throughout the cell cycle. The shift induced by the phosphorylation of the Cdc27 subunit of the anaphase-promoting complex (APC) was used as a marker of mitosis entry, whereas its dephosphorylation, which corresponds to cyclin B degradation, was used as a marker of the metaphase–anaphase transition (Kraft et al., 2003). Survivin, which is expressed at G2/M and declines at the G1 phase of the next cycle, was used as a second marker (Zhao et al., 2000). FACS analysis shows that mitosis exit starts 90 min after nocodazole release and that most cells have exited mitosis by 120 min. Our data show that Ran Ser135P is enriched upon mitosis entry and that dephosphorylation occurs late in mitosis, between 90 and 120 min, after anaphase onset but before survivin degradation (Fig. 3 A).

We then compared the subcellular localization of endogenous Ran Ser135P and active X-PAK4 during interphase (Fig. 3 B) and mitosis (Fig. 4). In interphase XL-2 cells, both Ran Ser135P and active X-PAK4 displayed a low and diffuse staining with visible enrichment in lamellipodia (Fig. 3 B, arrowheads). In addition, the Ran Ser135P species, and to some extent active X-PAK4, concentrated at the centrioles where they colocalized with polyglutamylated γ-tubulin stained by GT335 (Fig. 3 B, arrowheads; Bobinnec et al., 1998). A striking relocalization of both Ran Ser135P and X-PAK4 Ser533P occurred on chromatin as DNA started to condense during prophase. However, while active X-PAK4 decorated the entire condensing chromosomes, Ran Ser135P localized to more focused punctuate structures. In addition, both proteins colocalized with two strong dots, which are likely to be the centrosomes (Fig. 4). In metaphase, centrosome staining was increased for both the active X-PAK4 and Ran Ser135P. The chromatin staining evolved to metaphase plate decoration for active X-PAK4 and to more discrete substructures on the metaphase plate for Ran Ser135P (Fig. 4). At anaphase, the centrosomal staining of both proteins, although still visible, was much less intense, and chromosomal staining was lost for Ran Ser135P, but continued through anaphase A for active X-PAK4. Both proteins became associated with the midzone region of the

Published August 30, 2010

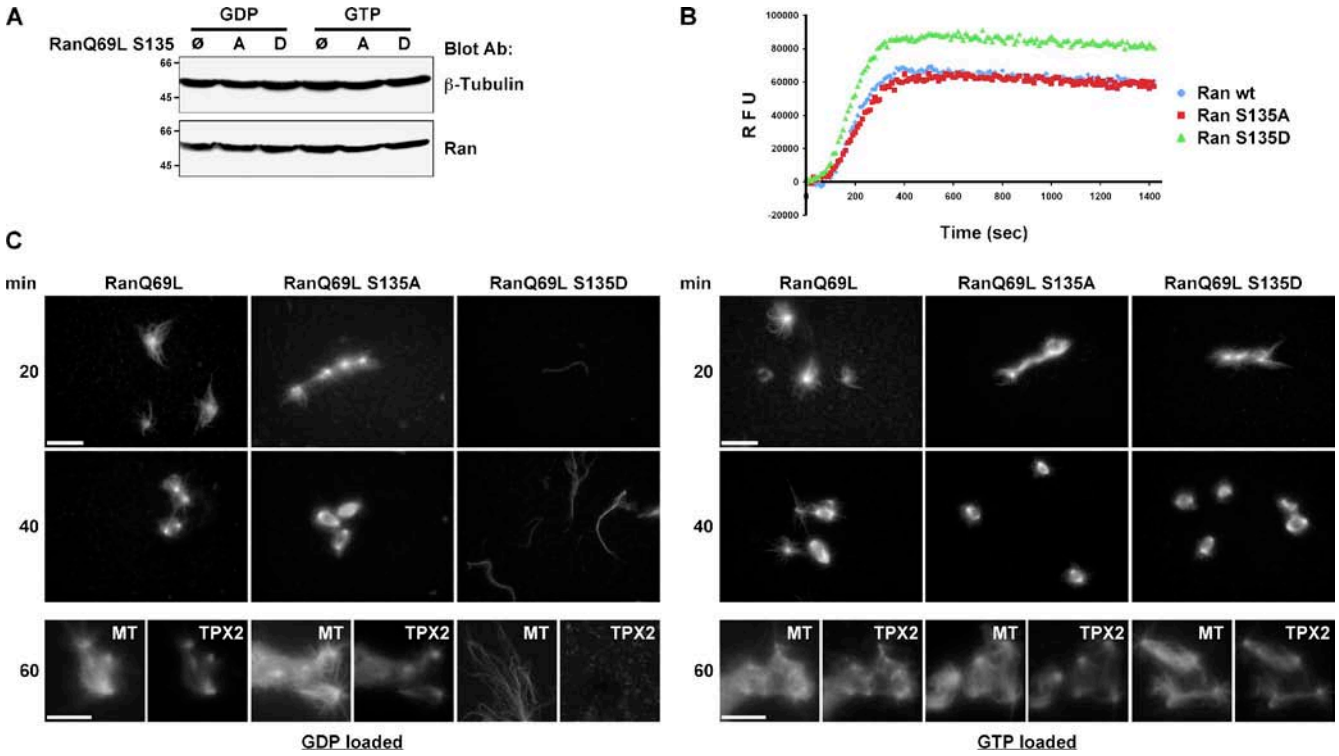

Figure 5. **The mutation of Ran serine-135 to aspartic acid (D) modulates the aster-promoting activity of GDP- but not GTP-bound RanQ69L.** Asters and mitotic spindle assembly after addition of 15 µM GDP- or GTP-bound RanQ69L or RanQ69L S135A or RanQ69L S135D mutants. (A) Immunoblot analyses of total extract for β-tubulin as loading control and Ran for recombinant Ran. (B) 1 µM GDP-loaded Ran wt, S135A, and S135D mutants were mixed with 1 µM MANT-GTP. Nucleotide exchange reaction was measured in relative fluorescence units (RFU) by FRET at 460 nm. (C, top) Representative micrographs of MT structures after indicated times. Bar, 25 µm. (Bottom) Same structures assembled after 60 min of incubation were costained for TPX2. Bar, 10 µm.

central spindle visualized by tubulin staining. Finally, during telophase, both proteins surrounded the midbody region (Fig. 4). Interestingly, Ran Ser135P also associated with the cortical contractile region, and was sometimes seen on unidentified filamentous substructures enveloping the anaphase spindle like a matrix (Fig. 4, anaphase A).

Altogether, our data show that the phosphorylation of Ran on serine-135 increases during mitosis and that active X-PAK4 and Ran Ser135P associate with similar substructures of the spindle, although chromosomal staining of Ran Ser135P is more restricted. This reinforces the significance of our finding that X-PAK4 phosphorylates Ran GTPase on serine-135.

A Ran serine-135 phosphomimetic mutant delays aster nucleation in *Xenopus* egg extracts

Because Ran Ser135P species associate with the spindle apparatus, we addressed its potential function in the regulation of spindle assembly.

To evaluate the function of Ran phosphorylation in the induction of MT asters, mutant Ran GTPases bearing either the Ser135-to-alanine substitution (S135A) to prevent phosphorylation or Ser135-to-aspartic acid substitution (S135D) to produce a phosphomimetic mutant were inserted in wild-type, Q69L, and T24N Ran backgrounds. GDP- or GTP-bound RanQ69L, Q69L S135A, and Q69L S135D double mutants were added to CSF extracts to follow MT nucleation. As seen by immunoblot analyses, the extracts were supplemented with the same amount of the different Ran mutants (Fig. 5 A). In the extract supplemented with GDP-bound RanQ69L and RanQ69L S135A, MT asters were induced as soon as 20 min after addition of the mutants, and these asters rapidly evolved into spindle-like structures (Fig. 5 C). In contrast, at the same time point, no mitotic asters were formed in the extract supplemented with GDP-bound RanQ69L S135D (Fig. 5 C). In the latter condition, microtubule polymerization finally started to occur after 30–40 min of incubation, and some masses of MTs that did not contain any obvious nucleation center were seen throughout the extract (Fig. 5 C). Later (after 60–80 min), asters finally started to organize properly (not depicted). Very similar results were observed when RanQ69L was added to a TPX2-depleted extract (not depicted). Quantification revealed that the addition of Ran Q69L S135A facilitates microtubule nucleation at early time points and the bipolarization of the asters into spindle-like structures at later time points (Fig. 6 A). In contrast, in RanQ69L S135D–containing extracts MT nucleation was considerably delayed, implying that SAFs were not properly activated (Fig. 6 A).

At this point, we wondered whether whether Ran phosphorylation on serine-135 might hinder GTP binding. To test this hypothesis, GTP loading was analyzed in vitro, using fluorescently labeled GTP (MANT-GTP; Klebe et al., 1993). Because, in the presence of Mg^{2+}, GDP and GTP are tightly bound to Ran (Görlich et al., 1996), nucleotide exchange of GDP-loaded Ran wt, S135A, and S135D mutants with MANT-GTP was initiated

Published August 30, 2010

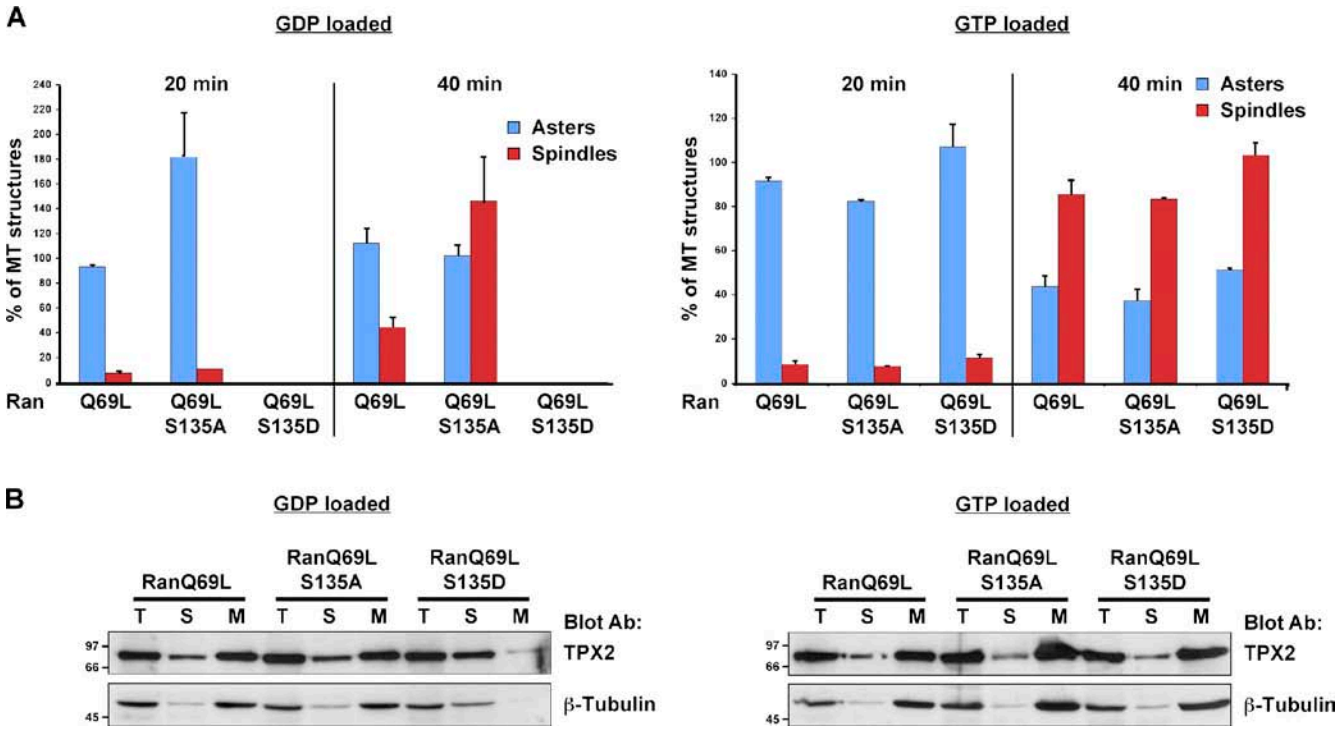

Figure 6. **The mutation of Ran serine-135 to aspartic acid (D) modulates the aster-promoting activity of GDP- but not GTP-bound RanQ69L.** (A) Quantification of MTs structures (asters and spindles), in RanQ69L GDP and RanQ69L GTP assays, described in Fig. 5, are respectively given an arbitrary 100% value at 20 min (n = 3, ±SD). (B) MT-associated proteins (MAPs) were purified after 40 min and TPX2 and β-tubulin levels were determined by immunoblot analyses in total extract (T), MAP-depleted extract (S), and MAP (M) fraction using specific antibodies.

by addition of EDTA, and measured as fluorescent intensity at 460 nm by FRET. GTP loading to Ran wt and S135A followed similar kinetics, whereas binding to Ran S135D was slightly facilitated (Fig. 5 B). The same results were obtained for the wt, S135A, and S135D Ran in a Q69L background (unpublished data). These results demonstrate that, in vitro, the GTP binding to Ran is not affected by mutations on serine-135.

GTP-bound mutants were then used in a MT aster assay, as above. In this condition, MT nucleation started as soon as 15 min after addition of the mutants, reflecting the fact that no nucleotide exchange in the extract is required (Fig. 5 C). Most importantly, no delay and even, reproducibly, a slight facilitation, was observed with the GTP-bound RanQ69L S135D mutant. Again, quantification confirmed these observations (Fig. 6 A).

The impaired function of GDP-bound RanQ69L S135D in the nucleation of MT asters was confirmed by the absence of TPX2, as seen by immunostaining of the MTs at 60 min, while TPX2 associated with the centers of asters and spindle poles induced by GDP- or GTP-bound RanQ69L and RanQ69L S135A and GTP-bound RanQ69L S135D (Fig. 5 C). To further confirm these morphological observations, we isolated MT-associated proteins (MAPs) from extracts supplemented with the Ran mutants and analyzed them for the presence of TPX2 and tubulin. TPX2 and tubulin were depleted from the supernatant during the MAP purification and recovered in the MAP fraction in all conditions except GDP-bound RanQ69L S135D extracts (Fig. 6 B). Thus, these biochemical data reinforce the microscopic observations that the activity of the RanQ69L Ser135 phosphomimetic mutant in aster nucleation depends on the nature of the bound nucleotide.

Serine-135 phosphorylation of Ran Q69L in extracto reproduces the inability of RanQ69L S135D to nucleate asters

To ensure that the effects in the extract of the serine-135 phosphomimetic mutation reproduce the PAK4-mediated phosphorylation of serine-135, we incubated a CSF extract with GDP- or GTP-RanQ69L in the presence of either GFP protein, as a control, or of constitutively active GFP-tagged PAK4 (PAK4/EN) kinase (Fig. 7 C, left). Induction of MT asters was analyzed after 20 and 40 min of incubation. Representative micrographs and quantification analyses are shown in Fig. 7, A and B. CSF-arrested extracts to which both GDP-bound RanQ69L and active PAK4 were added induced less than half as many MT asters as extracts to which GDP-bound RanQ69L and GFP were added (Fig. 7 B). These asters presented a lower number of nucleated MTs per aster and an overall larger surface, suggesting that MTs may be less dynamic (Fig. 7 A; unpublished data). Bipolarization, over the time course, was also delayed compared with the GFP control (Fig. 7 B). When using GTP-bound RanQ69L, the GFP-supplemented extract evolved a little faster than with the GDP-bound RanQ69L (as previously seen in Figs. 5 and 6). Addition of active PAK4 under these conditions did not inhibit aster nucleation and bipolarization, and in fact some facilitation was observed in several experiments (Fig. 7 A; unpublished data). Nonetheless, the overall surface of the asters remained larger than in the GFP-supplemented extract, but differences were not as important as in the GDP-bound Ran conditions.

Published August 30, 2010

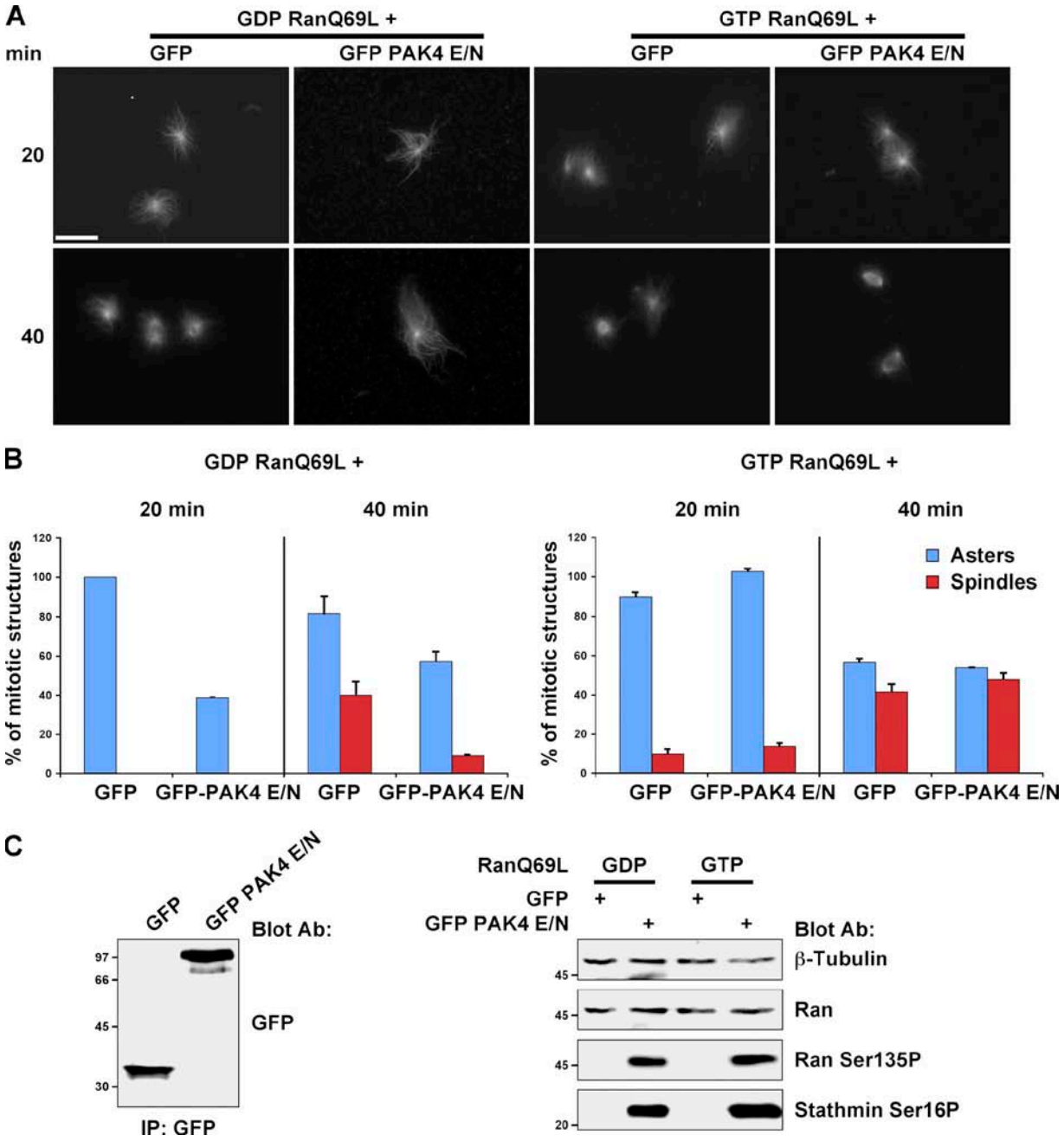

Figure 7. **Active PAK4-induced phosphorylation of RanQ69L regulates the MT structures induced by the GTPase.** Extracts were incubated for 15 min with GFP or GFP-tagged PAK4 E/N immobilized on protein-A Dynabeads prior aster assembly initiation by 15 µM GDP- or GTP-bound RanQ69L. (A) Representative structures observed at 20 and 40 min incubation. Bar, 25 µm. (B) Quantification of MT structures (asters or spindles) formed in the extracts as in A. GFP + GDP and GTP-bound RanQ69L conditions at 20 min are given an arbitrary 100% value. (n = 3, ±SD). (C) Extracts incubated for 40 min as in A were analyzed by immunoblotting for GFP and GFP-hPAK4 E/N (left pannel), phosphorylation of recombinant Ran proteins on serine-135 (Ran Ser135P), and of endogenous stathmin on serine 16 (Stathmin Ser16P; right panel). β-Tubulin demonstrates equal loading.

Immunoblot analyses of the extracts after a 30-min incubation confirmed that the active PAK4 induces phosphorylation of both GDP- or GTP-bound Ran on serine-135 (Fig. 7 C, right). Taken together, our results indicate that X-PAK4 activity no longer inhibits RanQ69L-induced MT nucleation when the GTPase is GTP bound. The overall stabilization of the MTs observed is more complex because it may be Ran dependent (Koffa et al., 2006; Silljé et al., 2006; Yokoyama et al., 2008) or result from a direct PAK4 regulation of MT stabilization/destabilization factors present in the extract. Indeed, we show here that inactivating phosphorylation of the endogenous stathmin on serine-16 is also induced by the active PAK4 in mitotic egg extract and is likely to participate in the observed stabilization of the MT asters (Fig. 7 C, right). In summary, our results show that promoting Ran phosphorylation on serine-135 by adding active PAK4 to mitotic extract inhibits RanQ69L-induced aster nucleation when GDP/GTP

Published August 30, 2010

exchange has not previously occurred, whereas phosphorylation of GTP-bound Ran slightly increases the nucleation capacity of RanQ69L.

Binding of Ran Q69L S135D phosphomimetic mutant to RCC1 is impeded

To obtain insight into the mechanism that prevents GDP-bound RanQ69L S135D from inducing aster formation, we studied whether phosphorylation of Ran could modulate its binding to some of the GTPase partners. Vectors expressing HA-tagged Ran mutants or HA tag only were transfected into HEK293 cells (Fig. 8). Equivalent amounts of HA-tagged Ran imunoprecipitates were analyzed by immunoblotting for the binding of the Ran GTPases to several known partners (Fig. 8, A and B). Wt, S135A, and S135D single-Ran mutants are mostly in a GDP-bound form in transfected cells because we could not detect interaction with importin-β and RanBP1, which only bind GTP-bound Ran (Fig. 8 A and Fig. S2 A). This was confirmed by the binding of NTF2 with the same efficiency to wt, S135A, and S135D mutants, whereas it was reported that NTF2 does not bind to RanT24N (Hughes et al., 1998). Accordingly, RCC1 immunoprecipitated with both wt and RanT24N, but not with RanQ69L. The S135A mutation did not affect RCC1 binding. In contrast, the S135D mutation abolished the Ran S135D single and T24N S135D double mutant binding to RCC1 (Fig. 8, A and B). Inhibition of GST-Ran Ser135D binding to RCC1 was also reproduced in vitro using purified recombinant proteins (Fig. S2 B). These results demonstrate that phosphorylation of Ran on serine-135, as mimicked by the S135D mutation, inhibits its binding to RCC1. The consequence of deficient RCC1 binding would potentially be a poor GTP loading of the Ran S135D mutant, a hypothesis which is supported by the observation that the RanQ69L S135D mutant binds the Ran-GTP partners, importin-β and RanBP1, with lower efficiency (Fig. 8 B). Interestingly, RanGAP1 behaved similarly to RCC1 toward Ran serine-135 phosphorylation, as it was immunoprecipitated with RanQ69L, but not with RanT24N, and with a small fraction of wt or S135A, but not S135D mutants (Fig. 8, A and B). This indicates that, although not detected with importin-β and RanBP1, a small fraction of wt and S135A mutants are GTP bound. Only the 90-kD sumoylated form of RanGAP1 was immunoprecipitated in these assays. Deficient binding of RanGAP1 to S135D was further confirmed in a Q69L background (Fig. 8 B). Using nocodazole-treated cells, we further verified that RCC1 phosphorylated in mitosis is not capable of binding Ran S135D. Interestingly, although HA-Ran wt becomes increasingly phosphorylated in mitosis, a decrease of its binding to mitotic, presumably phosphorylated, RCC1 was observed (Fig. S3)

Because Ran-GTP binding in the egg extract is mainly promoted by the guanine exchange factor RCC1, we wondered whether the GTP loading of the RanQ69L S135D mutant might be deficient in the extract. The addition of 2 µM RCC1 to CSF extract induces aster nucleation by activating endogenous Ran (Ohba et al., 1999). We reasoned that supplementing CSF extract with 2 µM RCC1 together with buffer or 15 µM Ran wt or S135A or S135D single mutants should primarily favor the GTP exchange toward the added recombinant Ran GTPases over the endogenous Ran. Fig. 8 C shows representative micrographs taken after 20 min of incubation. Only masses of disorganized MTs and rare huge asters were seen in the control and Ran S135D conditions, whereas numerous organized small asters were formed in the wt and Ran S135A conditions. The ratio of the mitotic figures formed in the wt and S135A reactions was over 10 times more than in control and S135D reactions (unpublished data). Thus, the extract containing Ran S135D behaves like the control extract. This implies that Ran S135D, unlike the wt and S135A Ran, cannot load GTP in the RCC1-supplemented extract.

To verify this hypothesis, RCC1-induced GTP loading was analyzed in vitro. GDP-loaded Ran wt, S135A, and S135D were mixed with MANT-GTP in the presence of RCC1 and nucleotide exchange was measured as previously (Fig. 8 D). In the presence of 0.1 µM RCC1, the relative fluorescence measured over time was similar for wt and S135A Ran, whereas almost no fluorescence was emitted with RanS135D, indicating that RCC1-induced GTP binding of Ran S135D is inhibited. GTP loading of wt and S135A Ran again increased over time in a similar manner with 0.2 µM RCC1, whereas at this concentration RCC1 only weakly promoted activation of Ran S135D.

Altogether, our data confirm that addition of GDP-bound RanQ69L S135D to the egg extract is unable to promote aster formation and that this loss of function results from an absence of GTP loading due to a poor RCC1 binding. In addition, because the Ran Ser135D mutation impedes the binding of the GTPase to RanGAP1, the PAK4 phosphorylated GTP-bound Ran, which is competent for nucleating MT asters, could potentially be protected against RanGAP1.

Inhibition of endogenous PAK4 delays mitosis

To determine a physiological function of Ran phosphorylation on serine-135 during the cell cycle, we silenced PAK4 by RNA interference in HeLa cells. A siRNA targeting the luciferase gene was used as a control (Luc). After a 48-h transfection, more than 90% of PAK4 was specifically depleted (Fig. 9 A). The Ran Ser135P to Ran ratio was similar in interphase for PAK4- and Luc-interfered cells, indicating that another kinase might be responsible for the generation of Ran Ser135P in interphase. In contrast, this ratio that increased by an average of twofold during mitosis with Luc siRNA (see also Fig. 3) only increasing by 1.2-fold with PAK siRNA and is therefore reduced by 70% in the absence of PAK4 (Fig. 9 B). A complete inhibition of Ran Ser135P was never observed, indicating that other mitotic kinases may also target this site. PAK4- and Luc-interfered cells were synchronized at the G2/M transition by RO3306. The mitotic index was determined upon RO3306 release as cells were allowed to proceed through mitosis. As seen in Fig. 9 C, after a 30-min release less than half of the PAK4-interfered cells had entered mitosis compared with controls. Over the time course this disability was not compensated, indicating that the loss of PAK4 expression induces a G2/M block rather than a delay. This was confirmed

Published August 30, 2010

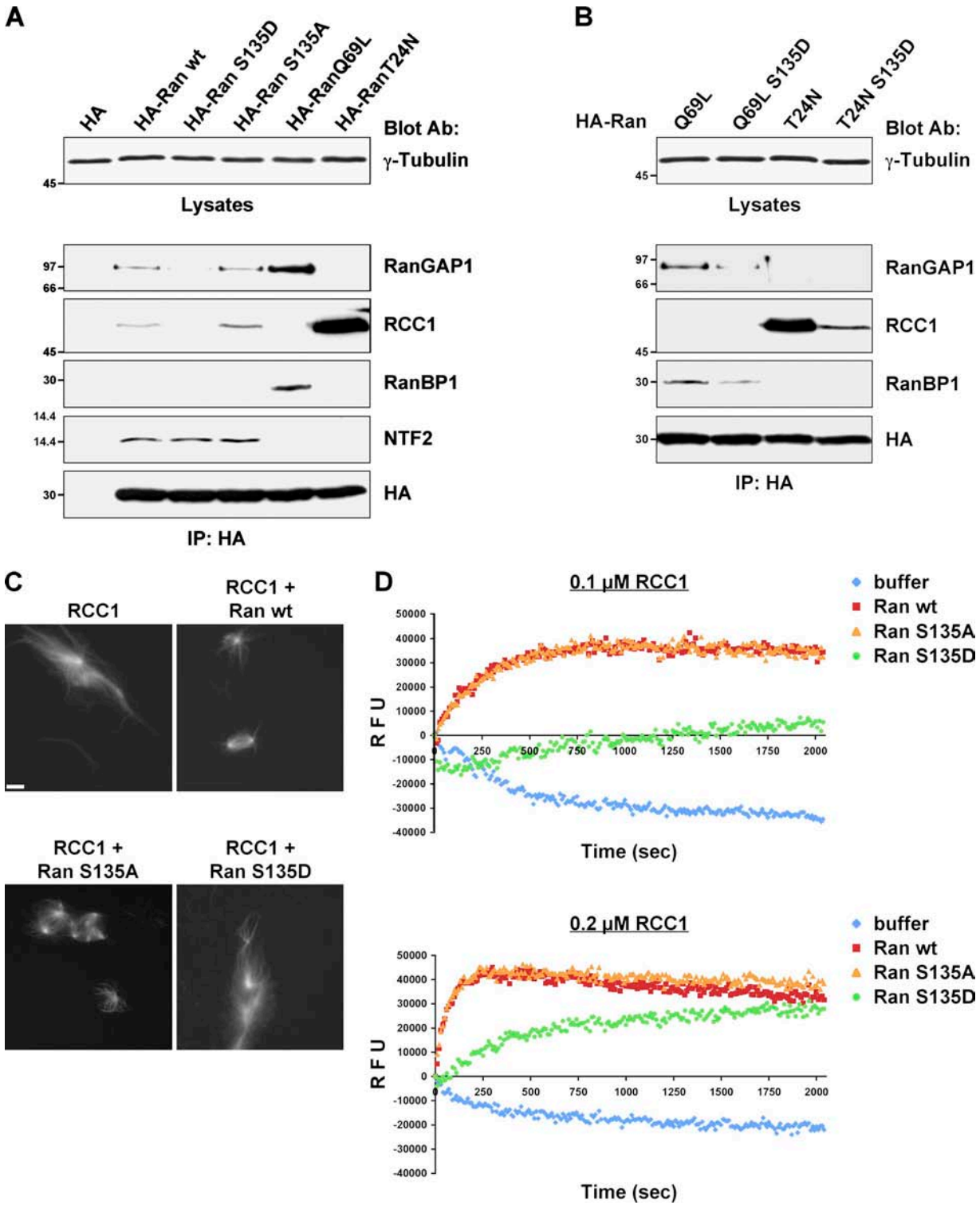

Figure 8. **RanGAP1 and RCC1 binding to Ran S135D are deficient.** (A and B) Whole cell lysates prepared from HEK293 cells transfected with the indicated HA-tagged Ran mutant constructs were immunoprecipitated using HA antibody. Total lysate and immunoprecipitates were analyzed by immunoblotting for the indicated proteins. (C) Representative MT structures observed 20 min after addition of 2 μM RCC1 in presence of buffer or 15 μM Ran wt, Ran S135A, or Ran S135D. Bar, 10 μm. (D) 1 μM GDP-loaded recombinant Ran wt, S135A, and S135D mutants were added to a mixture of recombinant RCC1 and 1 μM MANT-GTP. A representative experiment of the exchange reaction that was measured as described in Fig. 5 B ($n = 5$).

by performing time-lapse analyses upon RO3306 release (unpublished data) and by deriving the increase of the 2N cell population from FACS analyses, as also seen on representative micrographs at low magnification (Fig. 10 A). Finally, immunoblot analyses confirm the G2/M block because Cdc27 does not shift, while survivin expression remains low in PAK4-interfered cells compared with control upon RO3306 release (Fig. 10 B).

Published August 30, 2010

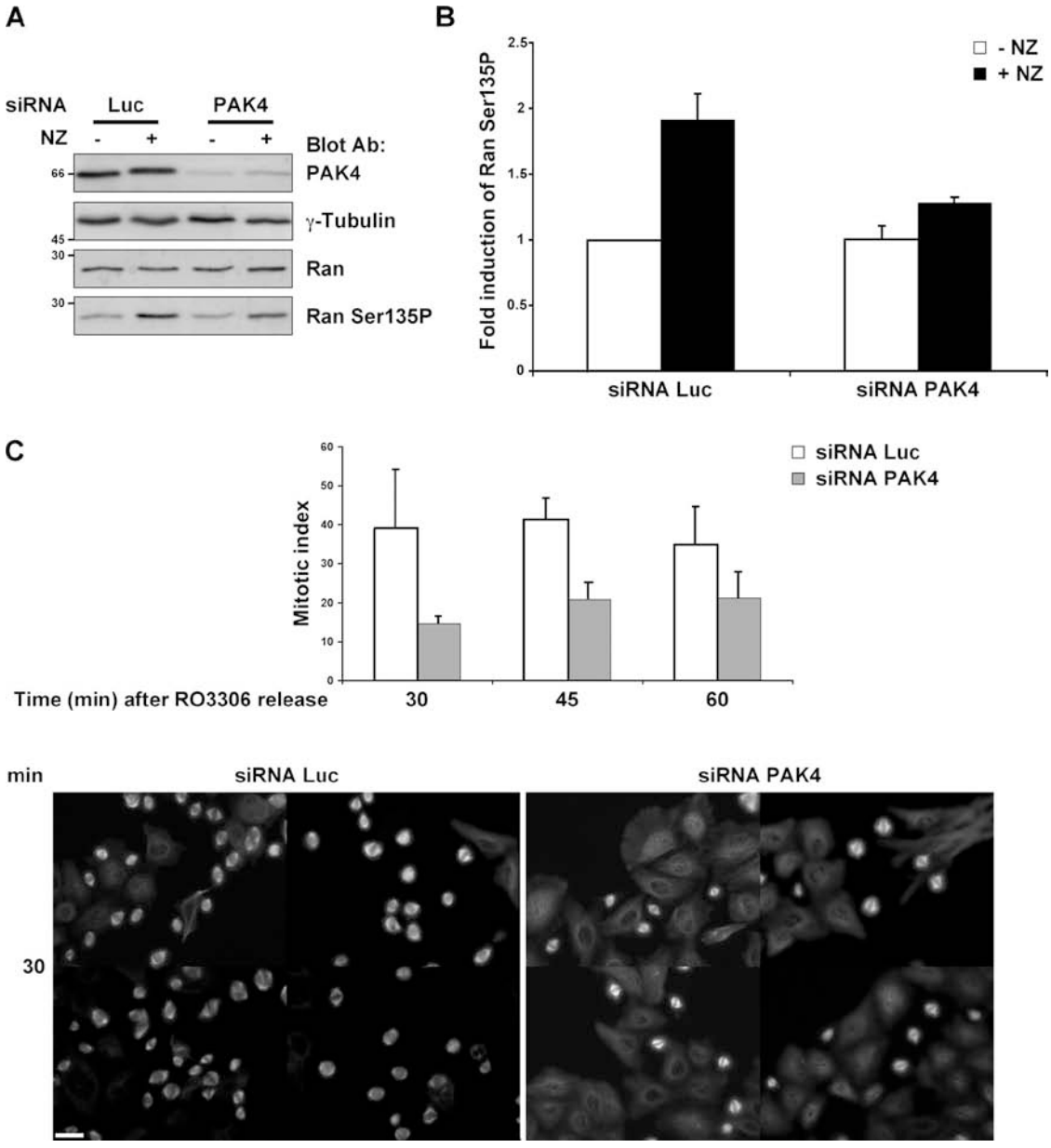

Figure 9. **PAK4 depletion induces a G2/M block.** (A) Representative immunoblot analyses of protein extracts from asynchronous (NZ−) or prometaphase-enriched (NZ+) HeLa cells transfected with luciferase or PAK4 siRNAs using indicated antibodies. (B) Quantification of Ran Ser135P present in the cells as in A ($n = 7$, ±SEM). (C) Mitotic index of PAK4- and luciferase-depleted cells after release from a G2/M block induced by RO3306 ($n = 3$, ±SEM) and four microscopic fields of β-tubulin staining of a representative experiment after 30 min release. Bar, 25 µm.

Discussion

At the onset of mitosis in somatic cells, the nuclear envelope breaks down, the interphase MT array depolymerizes, and mature centrosomes start to nucleate a large number of dynamic MTs. Mitotic kinase-mediated phosphorylation allows the sequential activation of both regulatory and structural proteins involved in the establishment of the mitotic spindle. In addition, Ran mediates MT nucleation and stabilization from chromosomes (Bastiaens et al., 2006; Clarke and Zhang, 2008; Torosantucci et al., 2008; O'Connell et al., 2009) and participates in centrosome-driven spindle assembly in somatic cells (Nachury et al., 2001; Ciciarello et al., 2004 ; Kaláb et al., 2006). Many partners of the Ran network are further regulated by phosphorylation during mitosis. In the present study, we demonstrate that Ran itself is subjected to a spatial regulatory phosphorylation in M phase.

X-PAK4 binds interphase and mitotic MTs and regulates interphase MT dynamics (Cau et al., 2001). In this paper, we demonstrate that GDP-bound RanQ69L-induced MT nucleation is increased in X-PAK4–depleted mitotic extract, and identify Ran as a novel PAK4 substrate and serine-135 as the unique phosphorylation site targeted. Ran serine-135 was previously proposed to be phosphorylated during mitosis by a Plk1-dependent mechanism (Feng et al., 2006). We demonstrate here that this site is a poor in vitro substrate for Plx1. Although we cannot rule out Plx1 involvement, we show that in human cells Ran

Published August 30, 2010

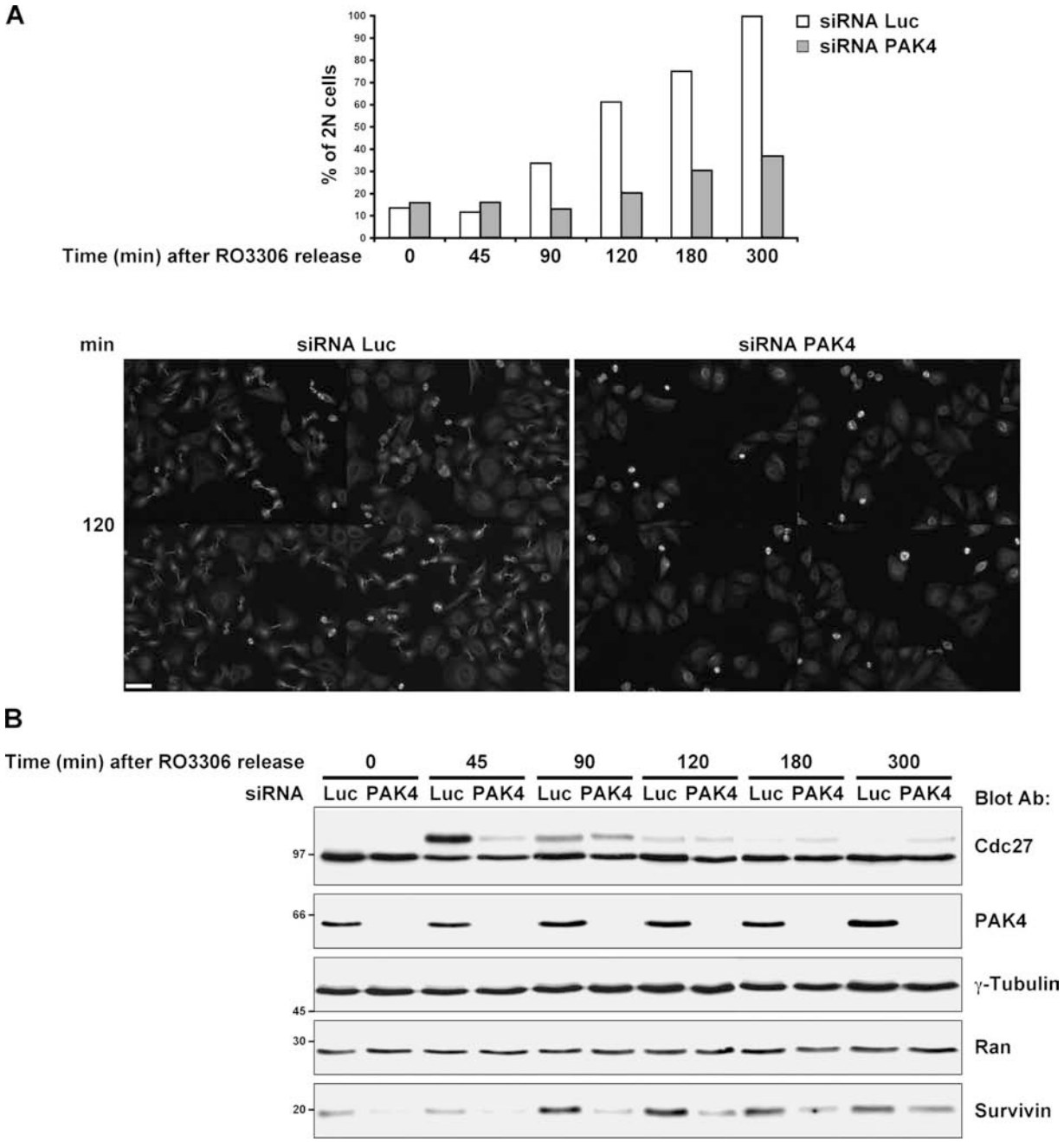

Figure 10. **PAK4 depletion induces a G2/M block.** (A) Percentage of 2N cells determined by FACS analysis fom a representative experiment (n = 4) described in Fig. 9 C and four microscopic fields of β-tubulin staining after 120 min release from the G2/M block. Bar, 50 µm. Number of 2N cells at 300 min in luciferase-depleted cells was given an arbitrary 100% value. A representative experiment, out of four independent experiments, is shown. (B) Total cell lysates from cells treated as described above were analyzed by immunoblot using indicated antibodies.

Ser135P increases during mitosis and that silencing of endogenous PAK4 efficiently, albeit not completely, decreases Ran Ser135P. In addition, PAK4 silencing induces a block at the G2/M transition, indicating that Ran Ser135P could be required early for mitosis entry.

Because silencing PAK4 in somatic cells probably prevents phosphorylation of different substrates, we developed assays based on RanQ69L-induced MT nucleation in CSF extract to get more insight into the functional importance of Ran phosphorylation on serine-135 during mitosis. We show that added GDP-bound RanQ69L S135D phosphomimetic mutant is strongly impaired in its capacity to promote MTs nucleation, whereas, and in contrast, in vitro GTP loading of the same mutant completely rescued and even slightly enhanced MT nucleation in the extract. Addition of active PAK4 to extract supplemented with GDP- or GTP-bound RanQ69L mimicked the above phenotypes, further supporting the functional importance of PAK4-mediated Ran phosphorylation. Because in vitro GTP loading of the S135D mutant was not affected, we wondered whether this mutant could impede the binding of the GTPase to some of its partners.

Ran serine-135 is a highly conserved residue from yeast to human that is located in a patch rich in lysine/arginine amino

Published August 30, 2010

acids (residues 129–141). Structural studies identify that RCC1 binding to Ran implicates the arginines at positions 134, 137, and 140 of Ran (Renault et al., 2001). Because PAK4-mediated phosphorylation at serine-135 creates an acidic charge in the basic patch, we speculated that it may also regulate the binding of RCC1 to this Ran interface. This would explain the GDP-bound defective phenotype we observed in CSF extracts. Indeed, RCC1-mediated GTP binding of Ran S135D in extracto did not activate MT aster nucleation. Furthermore, we show that GTP exchange induced by RCC1 in vitro is strongly impaired in the Ran S135D mutant compared with the wild type and S135A mutant.

Thus, depending on whether serine-135 phosphorylation occurs on GDP- or GTP-bound Ran, it could be inhibiting or slightly activatory. More importantly, we show that the Ran S135D mutant also does not bind efficiently to RanGAP1, a result that is in agreement with structural studies (Seewald et al., 2002). Although we did not analyze the consequence for GTP hydrolysis of the GTP-bound Ran Ser135D further, we hypothesize that, in the absence of binding to RanGAP1, the Ran Ser135P GTP-bound Ran could be locked into an activated state. Such a regulatory mechanism could allow fine tuning of Ran activity on the mitotic spindle. The subcellular localization of active X-PAK4 and Ran Ser135P during mitosis supports this hypothesis.

RCC1 dynamically mediates Ran GDP/GTP exchange during the cell cycle on the chromatin surface. Once GTP bound, the Ran–RCC1 binary complex dissociates from chromatin, allowing generation of new Ran-GTP on the chromatin (Li et al., 2003). X-PAK4 becomes activated on condensing chromatin during prophase and thus could phosphorylate the available (probably GTP-bound) Ran substrate that is in the vicinity of RCC1 on the chromosome surface. Phosphorylated Ran-GTP, which no longer binds RanGAP1, would then be protected against GTP hydrolysis. In such a context, complexes formed by interaction of GTP-bound Ran Ser135P with importin-β (and potentially other nuclear transport receptors) would be stabilized.

Such a mechanism could cooperate with the signaling pathways that, from prometaphase to metaphase, mediate chromatin-induced MT stabilization and spindle assembly. Among these, the CRM1/Ran-GTP–dependent localization of RanGAP1 and RanBP2 to the kinetochore (Arnaoutov and Dasso, 2005), the activity of the importin-β cargo HURP (Koffa et al., 2006; Silljé et al., 2006), and the CRM1-Survivin–mediated addressing of the chromosomal passenger complex to the centromere (Knauer et al., 2006) are highly dependent on Ran-GTP activity. During chromosome alignment Ran-GTP is required, but it must be strictly controlled because in egg extracts Ran also regulates the spindle checkpoint and too high a Ran-GTP level would abrogate the checkpoint (Arnaoutov and Dasso, 2003). Ran-GTP reaches its highest level when the checkpoint is released at the metaphase–anaphase transition. This transition correlates with an increase in the concentration of RCC1 (Arnaoutov and Dasso, 2003) and precedes the loss of chromosome-associated Ran Ser135P observed in anaphase A. Nevertheless, we cannot exclude that a fraction of GDP-bound Ran might also be phosphorylated before RCC1-mediated GDP/GTP exchange takes place, and if so could participate in the regulation of the GDP/GTP balance required for Ran activities on the spindle.

An increasing number of studies show that Ran is important for centrosome integrity and function. Although RCC1 is absent from the centrosome, Ran-GTP and RanBP1 are both present (Di Fiore et al., 2003; Keryer et al., 2003; Ciciarello et al., 2004; Torosantucci et al., 2008). Ran is a core component of the centrosome and interfering with the Ran pathway can lead to centrosomal defects (Di Fiore et al., 2003; Keryer et al., 2003), and delocalizing the centrosome-bound GTPase impedes centrosomal-mediated MT regrowth after nocodazole treatment (Keryer et al., 2003). *In Xenopus* egg extracts, Ran-GTP increases the nucleating capacity of centrosomes (Ohba et al., 1999; Carazo-Salas et al., 2001; Nachury et al., 2001). CRM1–Ran-GTP–NES protein complexes bring important cargoes that are required for centrosome function and integrity to the centrosomes (Keryer et al., 2003; Wang et al., 2005). In addition, the direct binding of survivin to Ran mediates TPX2 delivery to MTs in tumor cells (Xia et al., 2008). Thus, Ran is probably also subject to different regulatory mechanisms on the centrosome, although they are not yet understood. We propose that phosphorylation of Ran could confer protection to GTP-bound Ran against hydrolysis; it could then diffuse away, or be transported, from chromatin to the centrosomes, thus decreasing the Ran-GTP gradient. We are currently addressing the importance of Ran phosphorylation on serine-135 and trying to identify novel partners for these centrosomal activities, using purified cell culture–derived centrosomes and sperm chromatin-derived Ran–RCC1-depleted centrosomes.

A diffusible gradient of Ran-GTP emanating from the chromosomes, together with the specific subcellular localization of Ran partners, were shown to regulate multiple Ran functions during mitosis. We suggest that the array of Ran-dependent functions in centrosome integrity, K fiber–mediated chromosome capture, and the spindle checkpoint likely requires another level of regulation of Ran activity.

In the present study, we show that phosphorylation of Ran GTPase during mitosis regulates its binding to RCC1 and RanGAP1 and probably removes the GTPase from RCC1–RanGAP1 regulation. We propose that Ran phosphorylation could promote the stabilization of Ran complexes with nuclear transport receptors on the mitotic apparatus until dephosphorylation again allows RanGAP1, RanBP1/2 binding required for GTP hydrolysis and subsequent complex disassembly.

Materials and methods

DNA constructs

Vectors encoding His-tagged Ran wt, Q69L, and T24N (pQE-Ran wt, Q69L, and T24N mutants) were a gift from Dr. I. Vernos (Center for Genomic Regulation, Barcelona, Spain). Vectors encoding GST-tagged Ran wt and mutants were generated by PCR-based cloning into pGEX-4T1 (GE Healthcare). Corresponding cDNA were cloned into pRK5-HA vector (a gift from L.M. Machesky, Beatson Institute for Cancer Research, Glasgow, UK) for HA-tagged Ran's expression. Site-directed mutagenesis was performed using the QuikChange Site-Directed Mutagenesis kit (Agilent Technologies). Two vectors encoding constitutively active kinase X-PAK4 kinase were used: a GST-tagged X-PAK4 that only expresses the catalytic domain (aa 379–649) of the kinase (X-PAK4Ct) and a His-tagged construct that expresses the full-length kinase with two point mutations (S504E, S533N) that

Published August 30, 2010

renders it constitutive (X-PAK4/EN). Both constructs were described previously (Cau et al., 2001).

Vector encoding constitutively active GFP-tagged human PAK4 mutant (S445N, S474E) was generated by PCR-based cloning into pEGFP-C1 using pIRES2-EGFP hPAK4 S445N, S474E (gift from A. Minden, Rutgers University, Piscataway, NJ) as template. Human PAK6 was cloned by PCR from IMAGE clone 5170347 (GenBank/EMBL/DDBJ accession no. BC035596) and introduced into the pEGFP-C1 vector. The S531N mutation was introduced as previously described in order to generate a constitutively active mutant. Vectors encoding constitutively active GFP-tagged X-PAK1 (T403E) and X-PAK4 (S504E, S533N) mutants were described previously (Cau et al., 2001). Vectors encoding constitutively active GFP-tagged mouse PAK3 mutant (T421E) and human PAK5 (S573N) were a gift from J.V. Barnier and S. Cotteret (FRC 2118-CNRS, Paris, France). The vector encoding His-tagged RCC1 (pQE60-RCC1) was a gift from M.H. Verlhac (UMR 7622-CNRS, Paris, France). pRSET A vector encoding His-tagged stathmin was generated by PCR-based cloning from pCDNA3 Stathmin, a gift of Dr. A. Sobel (UMR 839-INSERM, France).

Antibodies

Rabbit polyclonal antibodies against GST-tagged *Xenopus* TPX2, His-tagged (human importin-β, RCC1, mouse RanGAP1), maltose binding protein (MBP) were raised and affinity purified at the CRBM animal facility. The construct for His-tagged human importin-β was a gift of Dr. Gorlich (ZMBH, Heidelberg, Germany; Kutay et al., 1997), GST-tagged *Xenopus* TPX2 construct was a gift of Y. Arlot (UMR 6061-CNRS, Rennes, France), His-tagged human RCC1 and mouse RanGAP1 constructs were gifts of M.H. Verlhac (Paris, France) and C. Janke (UMR 5237-CNRS, Montpellier, France), respectively, who also provided us with the mouse monoclonal antibody against polyglutamylated tubulin (GT335). Rabbit polyclonal antibodies against the active form of PAK4/5/6 and against X-PAK4 were described previously (Cau et al., 2001). Rabbit polyclonal antibodies against Cdc27 (Vigneron et al., 2009) were a gift from T. Lorca (UMR 5237-CNRS, Montpellier, France).

Ran Ser135P antibody was prepared at the CRBM animal facility by immunizing rabbits with the peptide (CRK VKA KS(PO_3H_2)I VFH RK) surrounding the phosphorylated Ran serine-135 sequence after coupling to thyroglobulin.

Antibodies directed against total Ran, RanBP1, HA (12CA5), Stathmin Ser16P that recognizes the stathmin protein phosphorylated on serine-16 were purchased from Santa Cruz Biotechnology, Inc. Antibodies against Poly-His and against GFP were from Sigma Aldrich and Torrey Pines Biolabs, respectively.

Protein expression and purification

Bacterially expressed GST-fused Ran wt, mutants, PAK4wt, and PAK4 catalytic domain were affinity purified using glutathione beads (GE Healthcare). After elution, recombinant proteins were dialyzed against 1x XB (100 mM KCl, 0.1 mM $CaCl_2$, 1 mM $MgCl_2$, 50 mM sucrose, and 10 mM Hepes, pH 7.7). For nucleotide exchange assay, recombinant proteins were GDP loaded by incubation in 10 mM Tris-HCl, pH 7.5, 100 mM KCl, 1 mM DTT, and 1 mM GDP before elution or trypsin cleavage. Loading was induced with 5 mM EDTA for 30 min at room temperature. Nucleotide was locked by the addition of 20 mM $MgCl_2$ for 5 min at room temperature. After elution or cleavage, recombinant GDP-loaded Ran proteins were dialyzed against exchange assay buffer (20 mM Tris-HCl, pH 7.5, 50 mM NaCl, and 5 mM $MgCl_2$). His-tagged Ran wt and mutants, statmin, as well as RCC1 were purified as described previously (Bompard et al., 2005). After elution, His-tagged Ran proteins and RCC1 were dialyzed against 1x XB and exchange assay buffer, respectively.

Cell lines, immunofluorescence, immunoprecipitation, and synchronization

Xenopus XL-2 cells were cultured at 27°C in Leibovitz's L-15/water (8:2) medium supplemented with 10% fetal bovine serum (FBS) and antibiotics. Human embryonic kidney 293 (HEK293) and HeLa cells were maintained at 37°C in DME supplemented with 10% FBS and antibiotics. Immunofluorescence experiments with XL-2 cells were performed as described previously (Bompard et al., 2008). In brief, secondary antibodies used were conjugated to Alexa 488 and 555 from Invitrogen. Cells were mounted in mowiol with anti-fading N-Propyl Gallate.

HEK293 cells were transfected using jetPEI (Polyplus-transfection; Ozyme) according to the manufacturer's instructions. 24 h after transfection, cells were lysed in MOPS-derived lysis buffer (50 mM MOPS, pH 7.2, 0.5% Triton X-100, 150 mM NaCl, 100 mM sodium phosphate, pH 7.2, 10 mM $MgCl_2$, 10 mM NaF, 1 mM Na_3VO_4, and protease inhibitor cocktail). Cleared lysates were either directly used for immunoblot analyses or immunoprecipitated by incubation with 12CA5 antibody cross-linked on protein A agarose beads (GE Healthcare) using dimethyl pimelimidate (DMP; Sigma-Aldrich) for 1 h at 4°C. Beads were extensively washed with lysis buffer before immunoblot analysis. To study the binding of wt Ran and mutants to various partners during mitosis, HEK293 transfected cells were either treated with vehicle or 500 ng/ml nocodazole for 14 h before lysis and immunoprecipitation. Immunoblots were processed with Photoshop CS2 software (Adobe) and quantified using ImageJ 10.2 software (NIH Image; http://rsbweb.nih.gov/ij/).

For synchronization in G1/S, HeLa cells were treated for 24 h with 2.5 mM thymidine. For synchronization in G2/M or prometaphase, Hela cells were released from thymidine block in medium containing 24 µM deoxycytidine (Sigma-Aldrich) and respectively 10 µM RO3306 (Calbiochem) or 40 ng/ml nocodazole (Sigma-Aldrich) for 14 h. Prometaphase-enriched cells were collected by shake-off. For quantification of mitotic cells, an average of 80 fields at 20x was acquired, for DNA and tubulin staining, using the scan slide function of MetaMorph software (MDS Analytical Technologies). Images of the resultant stacks were threshold and all nuclei, then all mitotic figures were counted using the integrated morphometry analysis function of MetaMorph software. These numbers were used to calculate the mitotic index.

RNA interference

siRNA were transfected into HeLa cells using Lipofectamine 2000 reagent (Invitrogen) as described previously (Bompard et al., 2008). Proteins were targeted with the following sequences: PAK4 with 5′-GGUGAACAUGUAUGAGUGU-3′ and Luciferase with 5′-CGUACGCGGAAUACUUCGA-3′. siRNA were purchased from Eurogentec. For evaluation of Ran Ser135P levels in prometaphase, 36 h after siRNA transfection cells were incubated in medium containing either vehicle or 100 ng/ml nocodazole for 14 h. Prometaphase-arrested cells were collected by shake-off and lysed in RIPA-derived lysis buffer (10 mM NaH_2PO_4, 100 mM NaCl, 5 mM EDTA, 1% Triton X-100, 0.5% NP-40, 80 mM β-Glycerophosphate, 1 mM DTT, 50 mM NaF, 1 mM Na_3VO_4, and protease inhibitor cocktail).

***Xenopus* egg extracts and MT structure nucleation assays**

Xenopus females were obtained from the CNRS breeding center located in Montpellier, France. Cytostatic factor (CSF) activity-arrested egg extracts were prepared as described previously (Cau et al., 2000). In brief, fresh eggs were dejellied in 2% cysteine (pH 7.8) and washed in XB buffer in the presence of 6 mM EGTA. Eggs were crushed at 20,000 *g* for 15 min, and the cytoplasmic layer was supplemented with an ATP regenerating system, cytochalasin B, and protease inhibitors, before use.

X-PAK4 or maltose binding protein control immunodepletion of the extracts were essentially performed as described previously (Hannak and Heald, 2006) using immunopurified antibodies. Usually 5 µg of immunopurified Abn122 antibodies (Cau et al., 2001) were used to immunodeplete endogenous XPAK4 from 150 µl of extract. One single round of depletion is sufficient to remove over 99% of the endogenous X-PAK4.

His- or GST-tagged recombinant Ran was added at 15 µM final concentration in the extracts. Both His- and GST-tagged proteins produced identical phenotypes and were used throughout this study. Recombinant His-tagged RCC1 was added at 2 µM final concentration.

GFP and constitutively active GFP-tagged hPAK4 E/N were purified from transfected HEK293 cells. In brief, 24 h after transfection cells were lysed in RIPA-derived lysis buffer. Clarified lysates were immunoprecipitated with GFP antibody for 1 h at 4°C followed by incubation with Dynabeads protein A for 30 min at 4°C. Beads were extensively washed in lysis buffer and 1x XB before use. One fifth of total immunoprecipitation was used per assay.

X-Rhodamine–labeled tubulin was prepared as described previously (Hyman, 1991). In all experiments X-Rhodamine–labeled tubulin was added to the extracts to a final concentration of 50 µg/ml.

Reactions were incubated at room temperature for indicated times. Aliquots of the reactions were snap-frozen in liquid nitrogen at different times during the experiment for Western blotting studies. For observation of Ran-induced MT structures, aliquots were fixed, spun onto coverslips through a glycerol cushion, and either directly mounted on slides with mowiol or processed for immunofluorescence as described previously (Hannak and Heald, 2006) using affinity-purified anti-TPX2 antibodies. For purifying the MAP fraction, 15 µl aliquots of the reactions were diluted in 200 µl of BRB80, 5 mM $MgCl_2$, 30% glycerol, layered over a cushion of BRB80, 5 mM $MgCl_2$, 40% glycerol, and spun for 20 min at room temperature and at 7,000 *g* in a microfuge. The supernatant was recovered, the interface of the cushion washed several times with buffer, and the pelleted MAP fraction resuspended for Western blot analysis.

Imaging and quantitative fluorescence analyses

Fixed cells and MT structures were viewed using an Axioimager Z1 (Carl Zeiss, Inc.) with either 10× EC Plan-Neofluar 0.3, 20× Plan-Apochromat 0.8, or 63× Plan-Apochromat 1.4 oil lenses (all from Carl Zeiss, Inc.). Micrographs were either collected using a CoolSnap HQ2 CCD camera (Roper Industries) driven by MetaMorph 7.1 software (MT structures) or using an Axiocam Mrm camera with a structured illumination model (apotome) driven by Axiovision software. Asters and spindles formed in the extract were quantified by manual counting of 40 fields at 20× using the manual count object function of MetaMorph software. Each experiment was repeated at least three times. Values are expressed as percentage; the total number of MT structures (asters plus spindles) in the control condition is given an arbitrary 100% value at each time point; error bars are the SD.

In vitro kinase assay

For Plx-1 and X-PAK4 activities, 0.3 µg of Plx1 purified from baculovirus (a gift from A. Abrieu, UMR 5237-CNRS, Montpellier, France) or GST-tagged kinase domain of X-PAK4 (X-PAK4 Cter) were incubated with the indicated Ran mutants (0.5 µg) or respectively dephosphorylated casein from bovine milk (0.3 µg; Sigma-Aldrich) or purified recombinant His-tagged stathmin (0.5 µg) for 20 min in 20 µl of kinase buffer containing 1 µl of 1 mM ATP and 0.5 µl of γ-[^{32}P]ATP. Reactions were loaded on 15% SDS-PAGE, transferred to PVDF membranes, and visualized by autoradiography.

Nucleotide exchange assay

For EDTA-induced Ran loading, 1 µM GDP-loaded Ran proteins (wt and mutants) were incubated with 1 µM MANT-GTP (Invitrogen) in loading buffer (30 mM potassium phosphate, pH 7.5, 5 mM $MgCl_2$, and 1 mM β-mercaptoethanol) for 10 min at room temperature before addition of 10 mM EDTA. Nucleotide exchange was monitored at ambient temperature as FRET at 460 nm after excitation at 290 nm using a POLARstar Omega (BMG Labtech) plate reader. For RCC1-induced Ran loading, 0.1 or 0.2 µM His-tagged RCC1 were incubated in loading buffer containing 1 µM MANT-GTP for 10 min at room temperature before addition of 1 µM GDP-loaded Ran proteins.

Flow cytometry

FACS analyses to determine cell DNA contents were performed as described previously (Bompard et al., 2008).

Online supplemental material

Fig. S1 shows that Ran is phosphorylated by subgroup II PAKs on serine-135. Fig. S2 shows that Ran partners binding to Ran mutants and that RCC1 binding to Ran is affected by S135D mutation in vitro. Fig. S3 shows a study of Ran binding to several partners during mitosis. Online supplemental material is available at http://www.jcb.org/cgi/content/full/jcb.200912056/DC1.

We thank Drs. Lorca, Abrieu, Gorlich, Vernos, Verlhac, Barnier, Cotteret, Machesky, and Arlot for the gift of reagents. We want to especially thank Dr. D. Fisher (IGMM, UMR 5535-CNRS, Montpellier, France), Dr. M. Dasso (National Institutes of Health, Bethesda, MD), and Dr. T. Spann (Northwestern University, Chicago, IL) for critical reading and editing of the manuscript. We thank the Montpellier RIO imaging facility.

G. Bompard is supported by a Contrat Jeune chercheur confirmé from INSERM. This work was supported by grants to N. Morin from the Association pour la Recherche sur le Cancer (ARC 3147) and from the Agence Nationale pour la Recherche GENOPAT.

The authors declare that they have no competing financial interests.

Submitted: 9 December 2009
Accepted: 6 August 2010

References

Arias-Romero, L.E., and J. Chernoff. 2008. A tale of two Paks. *Biol. Cell.* 100:97–108. doi:10.1042/BC20070109

Arnaoutov, A., and M. Dasso. 2003. The Ran GTPase regulates kinetochore function. *Dev. Cell.* 5:99–111. doi:10.1016/S1534-5807(03)00194-1

Arnaoutov, A., and M. Dasso. 2005. Ran-GTP regulates kinetochore attachment in somatic cells. *Cell Cycle.* 4:1161–1165.

Arnaoutov, A., Y. Azuma, K. Ribbeck, J. Joseph, Y. Boyarchuk, T. Karpova, J. McNally, and M. Dasso. 2005. Crm1 is a mitotic effector of Ran-GTP in somatic cells. *Nat. Cell Biol.* 7:626–632. doi:10.1038/ncb1263

Bastiaens, P., M. Caudron, P. Niethammer, and E. Karsenti. 2006. Gradients in the self-organization of the mitotic spindle. *Trends Cell Biol.* 16:125–134. doi:10.1016/j.tcb.2006.01.005

Bobinnec, Y., A. Khodjakov, L.M. Mir, C.L. Rieder, B. Eddé, and M. Bornens. 1998. Centriole disassembly in vivo and its effect on centrosome structure and function in vertebrate cells. *J. Cell Biol.* 143:1575–1589. doi:10.1083/jcb.143.6.1575

Bompard, G., S.J. Sharp, G. Freiss, and L.M. Machesky. 2005. Involvement of Rac in actin cytoskeleton rearrangements induced by MIM-B. *J. Cell Sci.* 118:5393–5403. doi:10.1242/jcs.02640

Bompard, G., G. Rabeharivelo, and N. Morin. 2008. Inhibition of cytokinesis by wiskostatin does not rely on N-WASP/Arp2/3 complex pathway. *BMC Cell Biol.* 9:42. doi:10.1186/1471-2121-9-42

Budhu, A.S., and X.W. Wang. 2005. Loading and unloading: orchestrating centrosome duplication and spindle assembly by Ran/Crm1. *Cell Cycle.* 4:1510–1514.

Callow, M.G., F. Clairvoyant, S. Zhu, B. Schryver, D.B. Whyte, J.R. Bischoff, B. Jallal, and T. Smeal. 2002. Requirement for PAK4 in the anchorage-independent growth of human cancer cell lines. *J. Biol. Chem.* 277:550–558. doi:10.1074/jbc.M105732200

Carazo-Salas, R.E., G. Guarguaglini, O.J. Gruss, A. Segref, E. Karsenti, and I.W. Mattaj. 1999. Generation of GTP-bound Ran by RCC1 is required for chromatin-induced mitotic spindle formation. *Nature.* 400:178–181. doi:10.1038/22133

Carazo-Salas, R.E., O.J. Gruss, I.W. Mattaj, and E. Karsenti. 2001. Ran-GTP coordinates regulation of microtubule nucleation and dynamics during mitotic-spindle assembly. *Nat. Cell Biol.* 3:228–234. doi:10.1038/35060009

Cau, J., S. Faure, S. Vigneron, J.C. Labbé, C. Delsert, and N. Morin. 2000. Regulation of *Xenopus* p21-activated kinase (X-PAK2) by Cdc42 and maturation-promoting factor controls *Xenopus* oocyte maturation. *J. Biol. Chem.* 275:2367–2375. doi:10.1074/jbc.275.4.2367

Cau, J., S. Faure, M. Comps, C. Delsert, and N. Morin. 2001. A novel p21-activated kinase binds the actin and microtubule networks and induces microtubule stabilization. *J. Cell Biol.* 155:1029–1042. doi:10.1083/jcb.200104123

Caudron, M., G. Bunt, P. Bastiaens, and E. Karsenti. 2005. Spatial coordination of spindle assembly by chromosome-mediated signaling gradients. *Science.* 309:1373–1376. doi:10.1126/science.1115964

Ciciarello, M., R. Mangiacasale, C. Thibier, G. Guarguaglini, E. Marchetti, B. Di Fiore, and P. Lavia. 2004. Importin beta is transported to spindle poles during mitosis and regulates Ran-dependent spindle assembly factors in mammalian cells. *J. Cell Sci.* 117:6511–6522. doi:10.1242/jcs.01569

Clarke, P.R., and C. Zhang. 2004. Spatial and temporal control of nuclear envelope assembly by Ran GTPase. *Symp. Soc. Exp. Biol.* 2004:193–204.

Clarke, P.R., and C. Zhang. 2008. Spatial and temporal coordination of mitosis by Ran GTPase. *Nat. Rev. Mol. Cell Biol.* 9:464–477. doi:10.1038/nrm2410

Di Fiore, B., M. Ciciarello, R. Mangiacasale, A. Palena, A.M. Tassin, E. Cundari, and P. Lavia. 2003. Mammalian RanBP1 regulates centrosome cohesion during mitosis. *J. Cell Sci.* 116:3399–3411. doi:10.1242/jcs.00624

Feng, Y., J.H. Yuan, S.C. Maloid, R. Fisher, T.D. Copeland, D.L. Longo, T.P. Conrads, T.D. Veenstra, A. Ferris, S. Hughes, et al. 2006. Polo-like kinase 1-mediated phosphorylation of the GTP-binding protein Ran is important for bipolar spindle formation. *Biochem. Biophys. Res. Commun.* 349:144–152. doi:10.1016/j.bbrc.2006.08.028

Goodman, B., and Y. Zheng. 2006. Mitotic spindle morphogenesis: Ran on the microtubule cytoskeleton and beyond. *Biochem. Soc. Trans.* 34:716–721. doi:10.1042/BST0340716

Görlich, D., N. Panté, U. Kutay, U. Aebi, and F.R. Bischoff. 1996. Identification of different roles for RanGDP and RanGTP in nuclear protein import. *EMBO J.* 15:5584–5594.

Gruss, O.J., R.E. Carazo-Salas, C.A. Schatz, G. Guarguaglini, J. Kast, M. Wilm, N. Le Bot, I. Vernos, E. Karsenti, and I.W. Mattaj. 2001. Ran induces spindle assembly by reversing the inhibitory effect of importin alpha on TPX2 activity. *Cell.* 104:83–93. doi:10.1016/S0092-8674(01)00193-3

Hannak, E., and R. Heald. 2006. Investigating mitotic spindle assembly and function in vitro using *Xenopus laevis* egg extracts. *Nat. Protoc.* 1:2305–2314. doi:10.1038/nprot.2006.396

Hughes, M., C. Zhang, J.M. Avis, C.J. Hutchison, and P.R. Clarke. 1998. The role of the ran GTPase in nuclear assembly and DNA replication: characterisation of the effects of Ran mutants. *J. Cell Sci.* 111:3017–3026.

Hyman, A.A. 1991. Preparation of marked microtubules for the assay of the polarity of microtubule-based motors by fluorescence. *J. Cell Sci. Suppl.* 14:125–127.

Joseph, J., S.T. Liu, S.A. Jablonski, T.J. Yen, and M. Dasso. 2004. The RanGAP1-RanBP2 complex is essential for microtubule-kinetochore interactions in vivo. *Curr. Biol.* 14:611–617. doi:10.1016/j.cub.2004.03.031

Kalab, P., and R. Heald. 2008. The RanGTP gradient—a GPS for the mitotic spindle. *J. Cell Sci.* 121:1577–1586. doi:10.1242/jcs.005959

Kalab, P., R.T. Pu, and M. Dasso. 1999. The ran GTPase regulates mitotic spindle assembly. *Curr. Biol.* 9:481–484. doi:10.1016/S0960-9822(99)80213-9

Kalab, P., K. Weis, and R. Heald. 2002. Visualization of a Ran-GTP gradient in interphase and mitotic *Xenopus* egg extracts. *Science.* 295:2452–2456. doi:10.1126/science.1068798

Kaláb, P., A. Pralle, E.Y. Isacoff, R. Heald, and K. Weis. 2006. Analysis of a RanGTP-regulated gradient in mitotic somatic cells. *Nature.* 440:697–701. doi:10.1038/nature04589

Keryer, G., B. Di Fiore, C. Celati, K.F. Lechtreck, M. Mogensen, A. Delouvee, P. Lavia, M. Bornens, and A.M. Tassin. 2003. Part of Ran is associated with AKAP450 at the centrosome: involvement in microtubule-organizing activity. *Mol. Biol. Cell.* 14:4260–4271. doi:10.1091/mbc.E02-11-0773

Klebe, C., T. Nishimoto, and F. Wittinghofer. 1993. Functional expression in Escherichia coli of the mitotic regulator proteins p24ran and p45rcc1 and fluorescence measurements of their interaction. *Biochemistry.* 32:11923–11928. doi:10.1021/bi00095a023

Knauer, S.K., C. Bier, N. Habtemichael, and R.H. Stauber. 2006. The Survivin-Crm1 interaction is essential for chromosomal passenger complex localization and function. *EMBO Rep.* 7:1259–1265. doi:10.1038/sj.embor.7400824

Koffa, M.D., C.M. Casanova, R. Santarella, T. Köcher, M. Wilm, and I.W. Mattaj. 2006. HURP is part of a Ran-dependent complex involved in spindle formation. *Curr. Biol.* 16:743–754. doi:10.1016/j.cub.2006.03.056

Kraft, C., F. Herzog, C. Gieffers, K. Mechtler, A. Hagting, J. Pines, and J.M. Peters. 2003. Mitotic regulation of the human anaphase-promoting complex by phosphorylation. *EMBO J.* 22:6598–6609. doi:10.1093/emboj/cdg627

Kutay, U., E. Izaurralde, F.R. Bischoff, I.W. Mattaj, and D. Görlich. 1997. Dominant-negative mutants of importin-beta block multiple pathways of import and export through the nuclear pore complex. *EMBO J.* 16:1153–1163. doi:10.1093/emboj/16.6.1153

Li, H.Y., D. Wirtz, and Y. Zheng. 2003. A mechanism of coupling RCC1 mobility to RanGTP production on the chromatin in vivo. *J. Cell Biol.* 160:635–644. doi:10.1083/jcb.200211004

Molli, P.R., D.Q. Li, B.W. Murray, S.K. Rayala, and R. Kumar. 2009. PAK signaling in oncogenesis. *Oncogene.* 28:2545–2555. doi:10.1038/onc.2009.119

Nachury, M.V., T.J. Maresca, W.C. Salmon, C.M. Waterman-Storer, R. Heald, and K. Weis. 2001. Importin beta is a mitotic target of the small GTPase Ran in spindle assembly. *Cell.* 104:95–106. doi:10.1016/S0092-8674(01)00194-5

Nakajima, H., F. Toyoshima-Morimoto, E. Taniguchi, and E. Nishida. 2003. Identification of a consensus motif for Plk (Polo-like kinase) phosphorylation reveals Myt1 as a Plk1 substrate. *J. Biol. Chem.* 278:25277–25280. doi:10.1074/jbc.C300126200

O'Connell, C.B., J. Loncarek, P. Kaláb, and A. Khodjakov. 2009. Relative contributions of chromatin and kinetochores to mitotic spindle assembly. *J. Cell Biol.* 187:43–51. doi:10.1083/jcb.200903076

Ohba, T., M. Nakamura, H. Nishitani, and T. Nishimoto. 1999. Self-organization of microtubule asters induced in *Xenopus* egg extracts by GTP-bound Ran. *Science.* 284:1356–1358. doi:10.1126/science.284.5418.1356

Renault, L., J. Kuhlmann, A. Henkel, and A. Wittinghofer. 2001. Structural basis for guanine nucleotide exchange on Ran by the regulator of chromosome condensation (RCC1). *Cell.* 105:245–255. doi:10.1016/S0092-8674(01)00315-4

Rennefahrt, U.E., S.W. Deacon, S.A. Parker, K. Devarajan, A. Beeser, J. Chernoff, S. Knapp, B.E. Turk, and J.R. Peterson. 2007. Specificity profiling of Pak kinases allows identification of novel phosphorylation sites. *J. Biol. Chem.* 282:15667–15678. doi:10.1074/jbc.M700253200

Seewald, M.J., C. Körner, A. Wittinghofer, and I.R. Vetter. 2002. RanGAP mediates GTP hydrolysis without an arginine finger. *Nature.* 415:662–666. doi:10.1038/415662a

Silljé, H.H., S. Nagel, R. Körner, and E.A. Nigg. 2006. HURP is a Ran-importin beta-regulated protein that stabilizes kinetochore microtubules in the vicinity of chromosomes. *Curr. Biol.* 16:731–742. doi:10.1016/j.cub.2006.02.070

Terry, L.J., E.B. Shows, and S.R. Wente. 2007. Crossing the nuclear envelope: hierarchical regulation of nucleocytoplasmic transport. *Science.* 318:1412–1416. doi:10.1126/science.1142204

Torosantucci, L., M. De Luca, G. Guarguaglini, P. Lavia, and F. Degrassi. 2008. Localized RanGTP accumulation promotes microtubule nucleation at kinetochores in somatic mammalian cells. *Mol. Biol. Cell.* 19:1873–1882. doi:10.1091/mbc.E07-10-1050

Vigneron, S., E. Brioudes, A. Burgess, J.C. Labbé, T. Lorca, and A. Castro. 2009. Greatwall maintains mitosis through regulation of PP2A. *EMBO J.* 28:2786–2793. doi:10.1038/emboj.2009.228

Wang, W., A. Budhu, M. Forgues, and X.W. Wang. 2005. Temporal and spatial control of nucleophosmin by the Ran-Crm1 complex in centrosome duplication. *Nat. Cell Biol.* 7:823–830. doi:10.1038/ncb1282

Wiese, C., A. Wilde, M.S. Moore, S.A. Adam, A. Merdes, and Y. Zheng. 2001. Role of importin-beta in coupling Ran to downstream targets in microtubule assembly. *Science.* 291:653–656. doi:10.1126/science.1057661

Wilde, A., and Y. Zheng. 1999. Stimulation of microtubule aster formation and spindle assembly by the small GTPase Ran. *Science.* 284:1359–1362. doi:10.1126/science.284.5418.1359

Wittmann, T., G.M. Bokoch, and C.M. Waterman-Storer. 2004. Regulation of microtubule destabilizing activity of Op18/stathmin downstream of Rac1. *J. Biol. Chem.* 279:6196–6203. doi:10.1074/jbc.M307261200

Xia, F., C.W. Lee, and D.C. Altieri. 2008. Tumor cell dependence on Ran-GTP-directed mitosis. *Cancer Res.* 68:1826–1833. doi:10.1158/0008-5472.CAN-07-5279

Yokoyama, H., O.J. Gruss, S. Rybina, M. Caudron, M. Schelder, M. Wilm, I.W. Mattaj, and E. Karsenti. 2008. Cdk11 is a RanGTP-dependent microtubule stabilization factor that regulates spindle assembly rate. *J. Cell Biol.* 180:867–875. doi:10.1083/jcb.200706189

Zhao, J., T. Tenev, L.M. Martins, J. Downward, and N.R. Lemoine. 2000. The ubiquitin-proteasome pathway regulates survivin degradation in a cell cycle-dependent manner. *J. Cell Sci.* 113:4363–4371.

Zhu, G., K. Fujii, Y. Liu, V. Codrea, J. Herrero, and S. Shaw. 2005. A single pair of acidic residues in the kinase major groove mediates strong substrate preference for P-2 or P-5 arginine in the AGC, CAMK, and STE kinase families. *J. Biol. Chem.* 280:36372–36379. doi:10.1074/jbc.M505031200